nature communications

Article

https://doi.org/10.1038/s41467-025-62416-3

Fasting is required for many of the benefits of calorie restriction in the 3xTg mouse model of Alzheimer's disease

Received: 30 October 2024

Accepted: 17 July 2025

Published online: 04 August 2025

Check for updates

Reji Babygirija[1,2,3], Jessica H. Han[3], Michelle M. Sonsalla[1,2,4], Ryan Matoska[1,2], Mariah F. Calubag[1,2,3], Cara L. Green[1,2], Anna Tobon[1,2], Chung-Yang Yeh[1,2], Diana Vertein[1], Sophia Schlorf[1,2], Julia Illiano[2,5], Yang Liu[1,2,6], Isaac Grunow[1,2], Michael J. Rigby[1,7,8], Luigi Puglielli[1,7,11], David A. Harris[2,5,9,11], John M. Denu[10,11] & Dudley W. Lamming[1,2,3,4,6,9,11,12]

Caloric restriction slows or prevents Alzheimer's disease in animal models. Calorie restriction is typically implemented in rodents through feeding once per day; as the animals quickly consume their food, they are subject to a prolonged self-imposed fasting period between meals. Here, we examine the distinct contributions of fasting and reduced calories to the beneficial effects of calorie restriction on Alzheimer's disease by placing male and female 3xTg and non-transgenic control mice on a series of diet regimens enabling us to dissect the effects of calories and fasting. We find that reducing calories alone improves body weight and glucose tolerance. However, a prolonged fast between meals is necessary for many of the benefits of calorie restriction, including improved insulin sensitivity, reduced Alzheimer's pathology, improved neuroprotective signaling, and improved cognition. Overall, our results suggest that both when and how much we eat may influence the development and progression of Alzheimer's disease.

The global population is rapidly graying; with this silver tsunami, the prevalence of Alzheimer's disease (AD) is increasing and by 2050, 13.8 million Americans are projected to be struggling with AD[1,2]. Decades of research to discover treatments for AD have been largely unsuccessful as well as extremely expensive; identifying new and cost-effective interventions that can delay or prevent AD is therefore of critical importance.

Caloric restriction (CR), a reduction in caloric intake without malnutrition or starvation, is the most robust, non-pharmacological and reproducible intervention for extending lifespan in model organisms[3]. CR slows the development of AD in multiple mouse models[4–7], as well as in squirrel monkeys[8]. While the impact of CR on AD in humans is mostly unknown, short-term CR can improve memory[9]. As few humans are prepared to engage in long-term CR, there is substantial interest in understanding the mechanisms underlying CR to harness its benefits without the need to subject individuals to an abstemious dietary regimen.

Many studies have investigated potential molecular mechanisms which may be engaged by a CR diet. To name just a few, CR decreases

[1]Department of Medicine, University of Wisconsin-Madison, Madison, WI, USA. [2]William S. Middleton Memorial Veterans Hospital, Madison, WI, USA. [3]Cellular and Molecular Biology Graduate Program, University of Wisconsin-Madison, Madison, WI, USA. [4]Comparative Biomedical Sciences Graduate Program, University of Wisconsin-Madison, Madison, WI, USA. [5]Wisconsin Surgical Laboratory in Metabolism, Department of Surgery, University of Wisconsin-Madison, Madison, WI, USA. [6]Endocrinology and Reproductive Physiology Graduate Program, University of Wisconsin-Madison, Madison, WI, USA. [7]Waisman Center, University of Wisconsin-Madison, Madison, WI, USA. [8]Neuroscience Training Program, University of Wisconsin-Madison, Madison, WI, USA. [9]University of Wisconsin Comprehensive Diabetes Center, Madison, WI, USA. [10]Department of Biomolecular Chemistry, University of Wisconsin-Madison, Madison, WI, USA. [11]Wisconsin Nathan Shock Center of Excellence in the Basic Biology of Aging, Madison, WI, USA. [12]University of Wisconsin Carbone Cancer Center, Madison, WI, USA. e-mail: dlamming@medicine.wisc.edu

mammalian target of rapamycin complex 1 (mTORC1) signaling and activates autophagy. We recently asked a different question based on the realization that CR-fed mice have an unusual feeding pattern. While *ad libitum* (AL)-fed mice eat in multiple small bouts throughout the day, with most of the intake during the night, CR regimens are performed by feeding mice only once-per-day. As a result, CR mice binge eat their food within 1–2 hours[10,11] and are subjected to a self-imposed ~22 hour fast between meals. We recently developed a series of feeding regimens that enabled us to dissect the relative contribution of fasting from energy restriction in the CR diet paradigm. We found that in wild-type mice, the prolonged fast between meals was necessary for the beneficial effects of a CR diet on metabolic health, frailty, longevity, and cognition[12].

In the present study, we expanded upon this work and set out to define the relative importance of fasting to the benefits of CR in AD. We used the 3xTg mouse model of AD, which expresses familial human isoforms of APP (APPSwe), Tau(tauP301L), and Presenilin (PS1M146V), and exhibits both Aβ and tau pathology as well as cognitive deficits[13]. 3xTg mice have been widely used to study geroprotective interventions, and CR has clearly beneficial effects on AD pathology and cognition in this model[4]. We placed 3xTg mice as well as non-transgenic (NTg) controls on a series of dietary regimens with similar compositions and investigated whether the benefits of CR on AD are mediated by energy restriction, fasting, or a combination of both.

Here, we find that fasting is not only required for many of the metabolic benefits of CR in the 3xTg mouse, but that it is also required for many of the molecular effects of CR, for CR-induced improvements in tau pathology and neuroinflammation, and for the full cognitive benefits of CR. Surprisingly, fasting is not required for CR-induced reductions in brain Aβ plaques accumulation in females, while CR had no effect on Aβ plaques in males. These results suggest that many of the beneficial effects of CR on memory, especially in males, may result from reduced tau pathology or altered molecular signaling, and not from the reduction in plaques. Our results demonstrate that fasting is a critical component of the benefits of CR on AD, suggesting that fasting alone or fasting-mimicking diets might help to prevent or delay AD in humans without requiring reductions in energy intake.

Results

CR has sex-specific effects on body composition and energy balance

We randomized 6-month-old male and female 3xTg and non-transgenic (NTg) control mice to one of three groups of equivalent body weight then placed each on one of three dietary regimens: *Ad libitum* (AL) - mice with free access to a normal rodent diet (Envigo Global 2018; Supplementary Data 1), Diluted *ad libitum* (DL) - mice with free access to Envigo Global 2018 diluted 50% with indigestible cellulose (TD.170950; Supplementary Data 1); equivalent to 30% restriction of calories without imposing fasting, and caloric restriction (CR) - mice fed a normal rodent diet (Envigo Global 2018) once per day in the morning, with 30% restriction of calories relative to AL-fed mice and with prolonged inter-meal fasting.

We followed the mice longitudinally for 9 months, tracking their body weight and determining their body composition at the beginning and the end of the experiment (Fig. 1A); as sex was a significant factor (3-way ANOVA, Supplementary Data 2) in the response of these outcomes and many other during the study, we analyzed the sexes separately. As we expected, neither CR nor DL-fed female 3xTg or NTg mice gained weight during the course of the experiment, while AL-fed females mice continued to gain weight (Fig. 1B, S1A); this was primarily the result of an effect of CR and DL-feeding on fat mass, which resulted in an overall reduction in adiposity in both the genotypes (Fig. 1C–E, S1B-D). We tracked food consumption rigorously and observed that both CR- and DL-fed mice had comparable calorie intake in both 3xTg and NTg's (Fig. 1F, S1E).

Similar to females, CR- and DL-fed NTg males maintained a lower bodyweight and adiposity than their AL-fed counterparts throughout the course of the study (Fig. S1F-I). However, while 3xTg males had an initial response in body weight to the diet regimens that was similar to the 3xTg females, as the experiment continued the CR-fed 3xTg males started to weigh more than the 3xTg DL-fed males (Fig. 1G), and by the end of the experiment AL- and CR-fed 3xTg males had comparable levels of fat mass, lean mass, and adiposity, while DL-fed 3xTg males had reduced fat mass and adiposity relative to both AL and CR-fed 3xTg males (Fig. 1H–J). As with females, CR and DL-fed 3xTg and NTg males had comparable reductions in calorie intake relative to AL-fed males (Fig. 1K, S1J).

CR-fed mice engage in rapid lipogenesis following refeeding and then sustain themselves with these stored lipids[14]. We can see these shifts in fuel utilization by using metabolic chambers to determine substrate utilization by analyzing the respiratory exchange ratio (RER), which is derived from oxygen consumption and carbon dioxide production. A high RER value signifies the utilization of carbohydrates for energy production or lipogenesis, while a value nearing 0.7 indicates that lipids serve as the primary energy source. As we anticipated, both male and female CR-fed 3xTg mice have a distinct RER curve from AL and DL-fed mice, reflecting the rapid induction of lipogenesis following feeding and a subsequent switch to utilizing lipids as the primary energy source (Fig. 2A, B, E, F). CR-fed 3xTg mice had decreased energy expenditure relative to AL-fed mice in both sexes; however, while DL-fed males had lower energy expenditure, this effect did not reach statistical significance (Fig. 2C, D, 2G, H).

Both male and female NTg mice fed a CR diet had similar RER patterns to those observed in 3xTg mice (Fig. S2A-B, E–F). DL-fed female and male mice had significantly higher energy expenditure relative to AL-fed mice in both sexes. Although CR-fed mice also exhibited lower energy expenditure, the difference was not statistically significant (Fig. S2C–D, G-H).

While CR-fed mice were provided food only at the beginning of the light cycle and ate quickly, we analyzed the feeding pattern of the AL and DL-fed mice while in the metabolic chambers. Across both genotypes and sexes, AL and DL-fed mice had similar patterns of eating, primarily consuming food during the dark cycle and with neither group undergoing fasting (Fig. S3A-D).

Improved glucose tolerance and insulin sensitivity is a hallmark of CR in mammals. We performed glucose and insulin tolerance tests (GTT and ITT, respectively), timing the assays such that mice in all groups were fasted for similar lengths of time. As anticipated, both CR and DL-fed female 3xTg and NTg mice had improved glucose tolerance relative to AL-fed mice (Fig. 3A, S4A). Strikingly, in agreement with our previous results in C57BL/6J mice, insulin sensitivity as assessed by an intraperitoneal ITT was significantly improved only in CR-fed female mice, and not in DL-fed female mice, regardless of genotype (Fig. 3B, S4B). We observed similar effects of CR and DL on glucose and insulin tolerance in male 3xTg and NTg mice (Fig. 3C, D, S4C, D).

Overall, we found that CR and DL-fed 3xTg and NTg mice of both sexes showed similar but not identical improvements in body weight and composition, as well as glucose tolerance. However, improvements in insulin sensitivity were observed only in CR-fed mice, demonstrating that as previously shown in wild-type mice, CR-induced improvements in insulin sensitivity require fasting (Fig. 3E).

Sex-specific effects of energy restriction with and without fasting on metabolism

To investigate potential differences and overlaps on the effects of energy restriction with and without fasting, we performed a targeted metabolomics analysis of plasma and brain of AL, CR, and DL-fed 3xTg mice of both sexes. Our analysis targeted ~50 metabolites across three molecular groups based on their chemical structures: amino acids, carbohydrates, and nucleosides/nucleotides.

https://doi.org/10.1038/s41467-025-62416-3

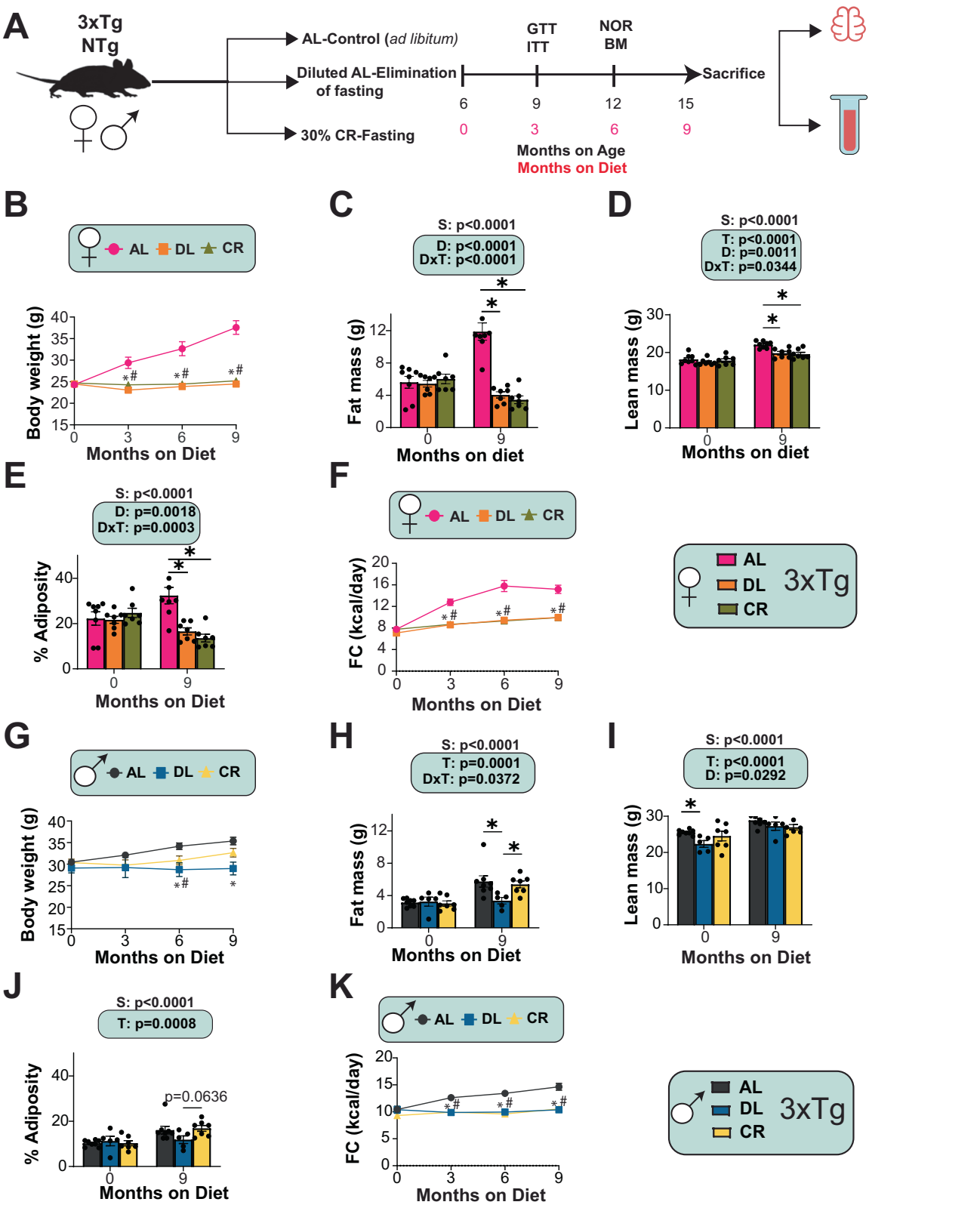

Principal Component Analysis (PCA) revealed distinct metabolic signatures in the plasma of AL, CR, and DL-fed 3xTg females (Fig. 4A). Plotting the 47 targeted plasma metabolites illustrates the shared and distinct metabolic signatures induced by CR and DL diets relative to AL-fed females (Fig. 4B, Supplementary Data 3-4). Among the significantly altered metabolites, we observed significant CR-induced increases in guanosine, leucine, and isoleucine, as well as CR-induced reductions in uridine. These changes were specific to CR and were not induced by a DL diet; while multiple metabolites trended in the same direction between CR and DL-fed mice, the only significantly altered metabolite that was shared in both CR and DL-fed mice was glucose-6-phosphate, which was decreased in the plasma of both groups (Figs. S5A-C). While broadly similar trends in metabolites appeared in male plasma metabolites, no metabolites reached statistical

Fig. 1 | Metabolic health outcomes of 3xTg-AD mice on different feeding regimens. A Experimental design: Six-month-old female and male 3xTg-AD and NTg mice were placed on either *ad libitum* (AL), Diluted AL (DL), or Caloric Restricted (CR, with fasting between once-daily meals) diet and phenotyped over the course of the next 9 months. **B**–**F** n = 8 AL, n = 7 DL and *n* = 7 CR fed 3xTg biologically independent female mice. **G**–**K** n = 8 AL, n = 5 DL, n = 7 CR 3xTg biologically independent male mice. **B**, **G**, **F**, **K** Two-way RM ANOVA followed by Dunnett's test vs. AL. *p < 0.05 AL vs DL, # p < 0.05 AL vs CR. **C**–**E**, **H**–**J** Statistics for the overall effect of diet (D), time (T), and the interaction (DxT) represent the p values from a two-way ANOVA; *p < 0.05 from a two-tailed Sidak's post-test examining the effect of parameters identified as significant in the two-way ANOVA. The overall effect of sex (S) represents the p value from a separately completed three-way ANOVA. **B** AL vs DL *$p = 0.003$, AL vs CR #$p = 0.0100$ (3 months), AL vs DL *$p = 0.0015$, AL vs CR #$p = 0.0022$ (6 months), AL vs DL *p < 0.0001, AL vs CR #$p = 0.0001$ (9 months). **C** AL vs DL *p < 0.0001, AL vs CR *p < 0.0001. **D** AL vs DL *$p = 0.0015$, AL vs CR *$p = 0.0004$ (**E**) Al vs DL *$p = 0.0002$, AL vs CR *p < 0.0001 (**F**) AL vs DL *$p = 0.0002$, AL vs CR #$p = 0.0005$ (3 months), AL vs DL *$p = 0.0005$, AL vs CR #$p = 0.0008$ (6 months) AL vs DL *$p = 0.0003$, AL vs CR #$p = 0.0005$ (9 months). **G** AL vs DL *$p = 0.0398$, AL vs CR #$p = 0.0493$ (6 months), AL vs DL *$p = 0.0148$ (9 months) (**H**) AL vs DL *$p = 0.0048$, DL vs CR *$p = 0.0237$ (**I**) AL vs DL *$p = 0.0450$ (**K**) AL vs DL *p < 0.0001, AL vs CR #p < 0.0001(3 months), AL vs DL *$p = 0.0030$, AL vs CR #$p = 0.0005$ (6 months), AL vs DL *$p = 0.0003$, AL vs CR #$p = 0.0007$ (9 months). Data represented as mean ± SEM. FC: Food Consumption. Source data are provided as a Source Data file.

significance, perhaps due to a smaller sample size (Fig. 4C, D, Supplementary Data 5-6).

Shifts in the levels of multiple metabolites within a single pathway can provide more information about regulatory processes than changes within levels of a single metabolite. We utilized Metabolite Set Enrichment Analysis (MSEA) to identify the distinct and shared pathways altered by each diet regimen. Our analysis identified multiple metabolic pathways that were altered in both 3xTg CR-fed and DL-fed females, including downregulation of pathways involving the metabolism of amino acids including "Cysteine and methionine metabolism", "Glycine, serine and threonine metabolism," and "Pentose phosphate pathway" (Fig. S5D, Supplementary Data 7). There were also pathways altered specifically by each diet in 3xTg females; CR-fed females showed upregulation of pathways including "Lysine degradation," and "Valine, leucine, and isoleucine degradation." Interestingly, DL-fed females had no significantly upregulated pathways, and indeed CR-fed females had upregulation of "Valine, leucine, and isoleucine biosynthesis," while DL-fed females had downregulation of this same pathway. As there were no significantly altered metabolites between the male diet groups, no pathways were significantly altered in DL-fed 3xTg males.

We also examined the metabolic signature in the whole brain of 3xTg male and female mice on each diet regimen. PCA on the identified 58 brain metabolites showed extensive overlap between female 3xTg mice fed any of the three diets (Fig. 5A, Supplementary Data 8). In particular, we were surprised to find that the effect of DL and CR diets on brain metabolites was virtually identical; a total of 21 metabolites were significantly altered by either the CR or DL diets or were altered in both. This included elevations in the levels of many essential and non-essential amino acids, including methionine and S-Adenosyl homocysteine (SAH), a metabolite in the cysteine and methionine metabolism pathway (Fig. 5B, S6A-C and Supplementary Data 9). Reflecting this high degree of overlap, MSEA found many biological pathways that were significantly affected by both DL and CR feeding in the brains of 3xTg female mice; pathways uniquely upregulated in CR-fed females included "Propanoate metabolism," "Folate biosynthesis," "Riboflavin pathway," "Lipoic acid metabolism," and "Tryptophan metabolism" (Fig. S7, Supplementary Data 10).

As in the brain, we observed many fewer changes in 3xTg males fed either the CR or DL diets than in females; however, PCA showed that CR was clearly distinct from both the AL and DL-fed groups (Fig. 5C and Supplementary Data 11). While there were similar trends in the effect of CR and DL diets on NAD metabolism (Fig. 5D and Supplementary Data 12), only NADP+ and ribulose-5 phosphate were significantly altered, and only in CR-fed 3xTg males (Fig. S8A-B). Among the significantly altered pathways in DL-fed 3xTg males were "Arginine and proline metabolism" and "Arginine biosynthesis" which may reflect the progression of neurodegeneration[15,16] (Fig. S7A, Supplementary Data 9). Notably, "Arginine biosynthesis" was similarly upregulated in both CR and DL-fed female 3xTg mice and approached significance in CR-fed male 3xTg mice (p = 0.066), the only pathway so similarly regulated in all four groups. In CR-fed mice, we found that "Glutathione metabolism," a key antioxidant defense pathway that has been shown to be altered in AD[17], was downregulated. The "Alanine, Aspartate and Glutamate metabolism" pathway, also previously implicated in AD[18,19], was also downregulated specifically in CR-fed males. Notably, the effect of CR and DL feeding on "Cysteine and Methionine metabolism" was observed in both plasma and brain samples of female, but not male, 3xTg mice, with similar effects on most of the metabolites detected despite the pathway being upregulated in the brain and downregulated in the plasma (Fig. S9A-B).

Fasting is required for CR-induced improvements in tau hyperphosphorylation and neuroinflammation, but not for CR-induced improvements in Aβ plaque deposition

To investigate the role of fasting in the ability of CR to attenuate AD pathology, we evaluated several pathological hallmarks of AD, including phosphorylation of tau, amyloid beta (Aβ) plaque deposition, and gliosis. In earlier studies[20], we did not see any visible plaques in 12-month-old 3xTg mice, and we therefore evaluated AD pathology in the cortex and hippocampus of both male and female 3xTg mice at 15 months of age. Brain sections from 15-month-old 3xTg mice females were immune stained and visualized using 3,3′-diaminobenzidine (DAB) (Fig. 6A). We observed significant plaque deposition in AL-fed females which was significantly diminished by both DL and CR, as shown by the reduced plaque area in both the cortex and hippocampus of female 3xTg mice fed these diets (Fig. 6A). However, upon immunoblotting for phosphorylated tau at phosphorylation site Thr231, we observed that only CR-fed mice had reduced tau phosphorylation, which reached statistical significance as compared to DL-fed mice (Fig. 6B). Furthermore, fluorescent immunostaining combined with quantitative analysis of cortical p-Tau Thr231 in female 3xTg mice also showed significant decrease in p-Tau only in CR-fed group (Fig. 6C).

As expected, the plaque-burdened AL-fed 3xTg females had significant neuroinflammation with higher levels of activated astrocytes (GFAP-positive) and microglia (IBA1-positive). CR-fed 3xTg females showed a significant reduction in both GFAP- and IBA1- positive cells (Fig. 6D). In contrast, despite a significant reduction in plaque burden, DL-fed 3xTg females did not show a reduction in the number of either GFAP or IBA1-positive cells (Fig. 6D).

Interestingly, in males, we did not observe significant plaque deposition as observed in females (Fig. S10A). However, CR-fed 3xTg males did showed a significant reduction in phosphorylated tau (Fig. S10B and S10C), as well as a significant reduction in IBA1 positive cells as compared to the AL-fed mice (Fig. S10D). Taken together, these results suggest that fasting is essential for reducing hyperphosphorylation of tau and gliosis in both females and males, independent of plaque deposition (Fig. 6E).

To gain further insight into neuroinflammation, we analyzed the expression of several inflammatory genes in the brains of both male and female 3xTg mice. We chose these pro-inflammatory and anti-

https://doi.org/10.1038/s41467-025-62416-3

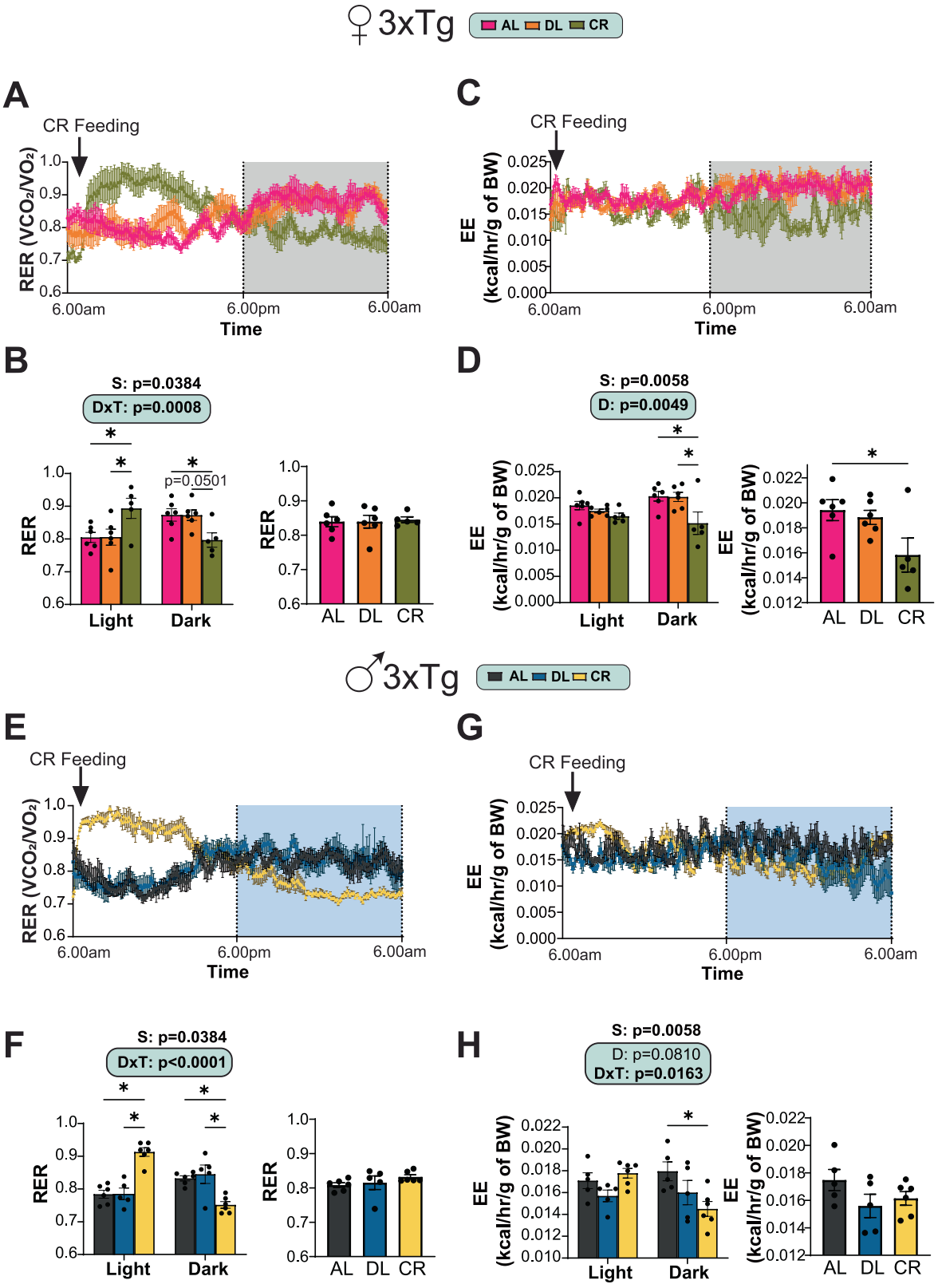

inflammatory genes based on prior studies demonstrating their relevance to AD-related neuroinflammation[21–24]. Interestingly, in DL fed 3xTg females, along with the activation of astrocytes and glia we found an increase in expression of inflammatory genes compared to AL-fed controls. Specifically, pro-inflammatory genes *Il6* and *Cxcl2* were elevated in DL-fed females, along with an increase in the gene *Il10* encoding the anti-inflammatory cytokine IL-10 (Fig. 7A, B), suggesting a mixed inflammatory response. In contrast, in 3xTg males, CR-fed mice had upregulation of both pro-inflammatory (*Il1b* and *Il6*) and anti-inflammatory (*Il10*) genes compared to AL- and DL-fed groups (Fig. 7C, D). A summary of the effects of diet (D), sex (S) and their interaction (DxS) for each gene separately is provided in Fig. 7E. We observed significant diet by sex interactions in pro inflammatory markers *Il1a, Il1b and Ccl2* genes.

Fig. 2 | Distinct fuel utilization patterns of 3xTg-AD mice under reduced caloric intake conditions. Metabolic chambers were used to determine fuel source utilization and energy expenditure 24 hours in female (**A**–**D**) and male (**E**–**H**). Six-month-old female and male 3xTg-AD mice were placed on either *ad libitum* (AL), Diluted AL (DL) or Caloric Restricted (CR with fasting between once-daily meals) diet and phenotyped over the course of the next 9 months. **A** Respiratory exchange ratio (RER) over 24hrs in females. (**B**) RER in light, dark and combined cycles in females. **C** Energy expenditure (EE) over 24 hrs in females. (**D**) EE normalized to body weight in females during light, dark and combined cycles in females. (**E**) RER over 24 hrs in males. (**F**) RER in light, dark and combined cycles in males (AL vs CR *p < 0.0001, DL vs CR *p < 0.0001 (light), AL vs CR *$p = 0.0016$, DL vs CR *$p = 0.0006$ (dark)). (**G**) EE over 24 hrs in males. (**H**) EE normalized to body weight in males during light, dark and combined cycles in males. **A**–**D** n = 6 AL, n = 6 DL and n = 5 CR-fed biologically independent 3xTg female mice were used. **E**–**H** n = 5 AL, n = 5 DL and n = 6 CR fed biologically independent 3xTg male mice were used. **B**, **D**, **F**, **H** (Left panel) Statistics for the overall effect of diet (D), time (T), and the interaction (DxT) represents the p values from a two-way ANOVA; *p < 0.05 from a two-tailed Sidak's post-test examining the effect of parameters identified as significant in the two-way ANOVA. The overall effect of sex (S) represents the p value from a separately completed three-way ANOVA. (Right panel) *p < 0.05, two-tailed Tukey's test post one-way ANOVA. Data represented as mean ± SEM. Source data are provided as a Source Data file.

CR and DL have distinct effects on mTORC1 signaling and autophagy

mTORC1 signaling has been extensively studied in the brains from AD mouse models, revealing mTORC1 activation in these brains[25,26]. It is widely believed that CR decreases mTORC1 signaling, which would result in the activation of autophagy while reducing overall biosynthesis, decreasing protein translation as well as lipid synthesis[27]. We therefore investigated how once-per-day CR and energy restriction alone impact mTORC1 signaling in the brains of the AD mice.

We performed immunoblotting in brain lysates to assess the phosphorylation of mTORC1 substrates p-S240/S244 S6 and T37/S46 4E-BP1. Compared to AL and DL-fed 3xTg females, we observed significantly decreased phosphorylation of both substrates in CR-fed 3xTg females (Fig. 8A–C).We assessed autophagy by examining expression of the autophagy receptor p62 (sequestosome 1, SQSTM1) and the autophagosome marker LC3A/B. We found that CR-fed female mice exhibited increased expression of both p62 and LC3A/B compared to AL and DL-fed groups (Fig. 8D, E). Although p62 accumulation is often associated with impaired autophagic flux, others who have observed increased levels of both p62 and LC3 following CR have interpreted this as enhanced autophagy induction[28]. In summary, these results indicate that fasting is critical for both CR-mediated suppression of mTORC1 signaling and CR-dependent induction of autophagy.

We also investigated the expression of brain-derived neurotrophic factor (BDNF), which is known for its neuroprotective effects; reduced BDNF levels are reported in the pathogenesis of AD[28–36]. BDNF has been shown to modulate mTORC1 signaling specifically in the neurons to promote synaptic plasticity and neuronal growth[37,38]. Moreover, CR has been shown to protect against cognitive decline via upregulation of BDNF[30,39]. In addition to the well-established benefits of CR, multiple studies have demonstrated that during intermittent fasting (IF), neurons undergo an adaptive response mediated by elevated BDNF levels, which enhance neuronal resilience and plasticity in response to metabolic stress[40–42]. Consistent with these findings, we find that BDNF levels were increased in the CR-fed 3xTg females compared to DL-fed mice ($p = 0.0808$); upregulation of BDNF may contribute towards the neuroprotective effects in the once-a-day fed CR group (Fig. 8F).

In males, we observed very similar results to those we found in females, with significant downregulation of p-S240/S244 S6 and T37/S46 4E-BP1 in the CR-fed group compared to the AL-fed group (Fig. 8G–I). While the DL-fed 3xTg males exhibited reduced phosphorylation of mTORC1 substrates compared to AL-fed males, these reductions were not statistically significant (Fig. 8G–I). Similar to females, we assessed the expression of autophagy markers p62 and LC3A/B. Although p62 levels were elevated in CR-fed mice compared to AL-fed controls, this difference did not reach statistical significance ($p = 0.0827$). In contrast, LC3A/B levels were significantly increased in CR-fed mice relative to AL and DL-fed groups (Fig. 8J, K). Finally, BDNF expression was significantly upregulated in CR-fed 3xTg males, which aligns with the improvements in AD pathology, particularly the tau-specific improvements in the males (Fig. 8L).

Fasting is required for rescuing hippocampal-dependent long-term memory in both sexes

We examined the contribution of fasting on CR-induced improvements in cognition by performing behavioral assays on 12-month-old 3xTg and NTg mice that had been fed either an AL, DL, or CR diet prior to sacrificing them for the histological assays described above. We examined the performance of both sexes in a Barnes Maze (BM) and tested Novel Object Recognition (NOR).

In the BM assay, mice were required to locate an escape box placed at the target hole using spatial cues during days 1-4 of the acquisition phase. On days 5 and 12 of the BM assay short-term memory (STM) and long-term memory (LTM), respectively, were tested, evaluating how well the mice remembered the location of the target hole. There was no effect of diet on the performance of NTg female mice in the BM, while there was an overall effect of diet on the BM performance of NTg males, with DL- and CR-fed NTg males performing better than AL-fed NTg males, especially in the STM assay (Fig. S11A-D, S11F-I).

Both AL- and DL-fed 3xTg female and male mice failed to locate the target hole within the given 90 seconds of assessment time even after 4 days of training (Fig. 9A, F). In contrast, CR-fed 3xTg mice of both sexes – but not DL-fed 3xTg mice - rapidly located the escape box during the training phase, during the STM test, and during the LTM test conducted 12 days after the initial assay (Fig. 9B, G). Additionally, AL-fed and DL-fed 3xTg mice of both sexes made more errors during the training phases than CR-fed mice (Fig. 9C, D, H, I).

The NOR task evaluates the preference for exploring a familiar object versus a new object and is quantified based on a discrimination index (DI). A positive DI implies a preference for exploring novelty, indicating that the memory of the familiar object persists and that the mice favor exploring the new object. As expected, NTg female mice fed any of the three diets performed well at the NOR test with a positive DI and no difference between groups (Fig. S11E). In contrast while male NTg mice didn't show significant deficits in STM, the CR-fed males performed better during the LTM test then DL-fed males (Fig. S11J).

We found that AL-fed 3xTg females spent more time with the familiar object than the novel object, suggesting defects in recognition memory (Fig. 9E). However, both the DL fed, and CR-fed females spent more time with novel objects than with the familiar object (Fig. 9E). However, 3xTg males did not show significant changes in their discrimination index, although CR-fed 3xTg males had the highest DI during the LTM test (Fig. 9J). Overall, these results demonstrate that fasting plays a role in the cognitive benefits of a CR diet for 3xTg mice of both sexes.

Fasting promotes survival outcomes in 3xTg AD-mice

Throughout our experiments, and consistent with our previous findings[20] as well as studies by other groups, we observed that 3xTg mice, particularly males, had a higher mortality rate as they approached one year of age. While we did not intend originally intend to assess the effects of these diets on survival, in agreement with these previous results, we found that AL-fed 3xTg males have a shorter lifespan than AL-fed female mice (Fig. S12A-B). 3xTg males fed a DL diet had significantly

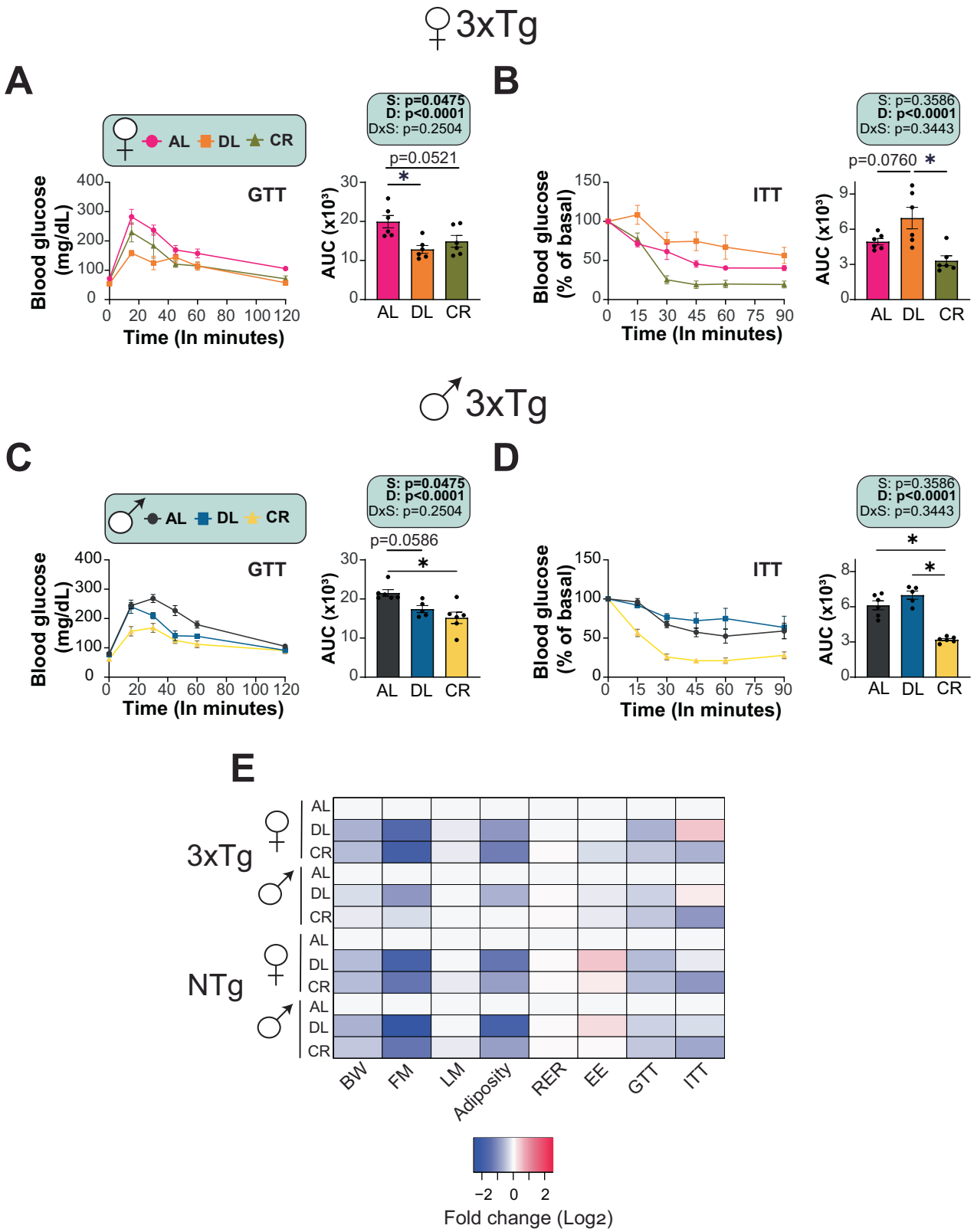

decreased survival (log-rank test, p = 0.009) relative to AL-fed males (Fig. S12B). In contrast, female 3xTg mice did not show significant differences in survival between the different dietary groups (Fig. S12A).

Discussion

There has been growing interest in dietary interventions for diseases of aging, including AD[43]. One such possible intervention is fasting, which has shown potential promise as an effective intervention in alleviating symptoms of neurodegenerative diseases including AD and Parkinson's disease[44–47]. Previous studies have found benefits of intermittent fasting without calorie restriction in mice, finding that intermittent fasting improved glucose metabolism, regulates circadian rhythms, and promotes neuronal resilience as well as recovery from neural injury[48–51]. In the context of AD, CR or intermittent fasting

Fig. 3 | Fasting is required for CR-induced insulin sensitivity in both female and male 3xTg-AD mice. Glucose (**A**) and insulin (**B**) tolerance tests were performed in female mice after three months on *ad libitum* (AL), Diluted AL (DL) or Caloric Restricted (CR with fasting between once-daily meals) fed diets. **A** GTT: n = 6 3xTg biologically independent mice per group. **B** ITT: n = 6 3xTg biologically independent mice per group. Glucose (**C**) and insulin (**D**) tolerance tests were performed in male mice after three months on AL, DL or CR fed diets. **C** GTT: n = 6 AL, n = 5 DL and n = 6 CR fed 3xTg biologically independent mice. (**D**) ITT: n = 6 AL, n = 5 DL and n = 6 CR fed biologically independent mice. **E** Heat map representation of all the metabolic parameters in 3xTg and NTg female and male mice. Color represents the $\log_2$ fold-change vs. AL fed mice. **A**–**D** Statistics for the overall effects of diet (D), sex (S) and their interaction (DxS) represent the p values from a 2-way ANOVA; *p < 0.05, from a two-tailed Tukey's test post ANOVA. **A** AL vs DL *$p = 0.0065$. (**B**) DL vs CR *$p = 0.0018$. (**C**) AL vs CR *$p = 0.0030$. (**D**) AL vs CR, DL vs CR *p < 0.0001. Data represented as mean ± SEM. NTg, Non-transgenic control, AUC, Area Under the Curve. Source data are provided as a Source Data file.

independently has been shown to promote cognitive function and protect from worsening AD pathology in animal models of AD[4–8,45,46,52,53]. However, the physiological and molecular mechanisms that underlie the benefits of CR on cognition – as well as its beneficial impacts on the development and progression of Alzheimer's disease – have remained elusive.

Recent work from our lab and others has demonstrated that in wild-type mice, many of the benefits of CR arise not from the reduction in calories, but instead from the prolonged fasting period that accompanies once-a-day experimental CR regimen. Fasting in the context of CR is required for the benefits on insulin sensitivity, frailty, cognition, and lifespan in wild-type mice[12,54], and indeed fasting alone without reduction of calories is sufficient for many of the molecular effects of CR as well as extending lifespan in wild-type mice[12,55].

Here, we build on this foundation by determining if the protective effects of CR on the progression and development of AD arise from the restriction of energy alone or as a result of fasting between meals. We placed both female and male 3xTg AD and NTg mice on different feeding regimens allowing us to distinguish between the effects of energy restriction and fasting. Metabolic and behavioral phenotyping was performed in both genotypes; however, molecular and histological analysis was conducted only in the 3xTg-AD group. In 3xTg AD mice, we found that a reduction of calories without a prolonged fast improves glucose tolerance and aspects of AD pathology, reducing the density of Aβ plaques and neuroinflammation, but did not improve tau pathology. In contrast, prolonged fasting was necessary for CR-mediated improvements in insulin sensitivity and tau pathology.

Without exception, CR with fasting had equal or greater cognitive benefits in multiple assays and in both sexes of 3xTg AD mice than energy restriction alone. Fasting was likewise required for CR-mediated molecular changes, including CR-induced reduction in brain mTOR signaling and the activation of autophagy. While there were sex-specific effects of CR, the importance of fasting largely held true across both sexes. Our results suggest that prolonged fasting between meals is an essential component of the benefits of CR on the development and progression of AD in mice.

CR-mediated attenuation of Aβ plaques been demonstrated in various AD mouse models[5,7,56]. Further, a previous study, found that CR reduces both Aβ and tau accumulation and improved cognitive performance in the 3xTg mouse model of AD[4]. Our findings are consistent with these previous reports, as we observed attenuation of Aβ plaques and tau pathology in CR-fed 3xTg mice.

Importantly, we have gained new insight into the mechanisms behind the benefits of a CR diet. First, DL-fed mice, which were energy restricted but did not experience prolonged daily fasts, showed significant attenuation of Aβ plaques. Notably, this occurred in the absence of improved insulin sensitivity, neuroinflammation, brain mTORC1 signaling, or activation of brain autophagy – all physiological and molecular changes that have been hypothesized to explain the ability of CR to slow the development or promote the clearance of Aβ plaques. Moreover, while DL-fed mice did show a trend towards cognitive improvements, it was clearly not as beneficial as CR. The modest benefits of targeting Aβ plaques alone may help explain the only partial success of Aβ-targeted antibodies in slowing cognitive decline in humans with AD[57,58].

The importance of fasting for the cognitive response to CR was evident in behavioral assays. 3xTg mice have consistently been shown to have impairments in hippocampal-dependent tasks such as Barnes Maze and NOR with memory deficits becoming apparent as early as 4-6 months of age and growing more severe with increasing age[13,59]. Here, we found that CR-fed 3xTg mice, which underwent prolonged daily fasting, had significantly better spatial reference memory compared to both AL-fed and DL-fed 3xTg mice. This was particularly evident with regards to latency to target in both males and females. Latency to target measures how fast the mouse reaches the correct escape hole after learning its location during the training phase, which is determined by how well they can recall the correct location, and thus mostly reflects spatial reference memory. In contrast, error hole visits provide insights into search strategy; entries into non-target holes are considered to be errors in working memory[60–64]. The findings from our study suggest that mice subject to energy restriction with fasting (CR) have significantly better spatial reference memory than mice subject to energy restriction without fasting (DL).

Overall, our results demonstrate that, energy restriction with fasting – traditional once-per-day CR – was highly effective in improving cognition, reducing not only Aβ plaques but also hyperphosphorylation of tau and tau pathology, reducing neuroinflammation, and was accompanied by molecular changes believed to be beneficial, notably the reduction of mTORC1 signaling and activation of autophagy. In combination with our results in DL-fed mice, we conclude that prolonged fasting between meals is, at a minimum, required for most of the benefits of CR except the reduction of Aβ plaques.

Rather surprisingly, this suggests that the benefits of reduced mTORC1 signaling, and increased autophagy may be mediated primarily by an Aβ-independent mechanism and moreover, previous studies have demonstrated that mTORC1 inhibition leads to the suppression of tauopathy[65,66]. These findings are consistent with studies in transgenic mouse models of tauopathies, where CR has been shown to alleviate tau pathology and improve cognitive function[67–70]. Intriguingly, despite DL reducing plaque deposition, astrocytic and microglial activation in the DL mice was comparable to AL-fed mice, while pro-inflammatory gene expression was extremely high. In contrast, CR-fed females not only had reduced plaques, but had reduced glial activation relative to both CR and DL-fed mice, with substantially lower pro-inflammatory gene expression, suggesting that while caloric reduction alone may attenuate plaque pathology, the reduction in plaque deposition observed in the DL-fed mice may not be mediated by glial cells. Further, it suggests that the inflammatory response is also independent of plaque burden. Future studies utilizing spatial transcriptomics or single-cell nucleus RNA sequencing will be critical to determine whether these inflammatory patterns persist at the regional and cellular levels. Throughout our study, we observed largely similar physiological, molecular and behavioral outcomes in response to all the three feeding regimens in both sexes with the exception in neuropathological outcomes. Specifically, the reduction of calories with or without fasting resulted in sex specific reduction of Aβ plaques in both cortex and hippocampus. While DL and CR reduced plaque deposition in both regions in females, there was no effect of either DL or CR on plaques in males.

https://doi.org/10.1038/s41467-025-62416-3

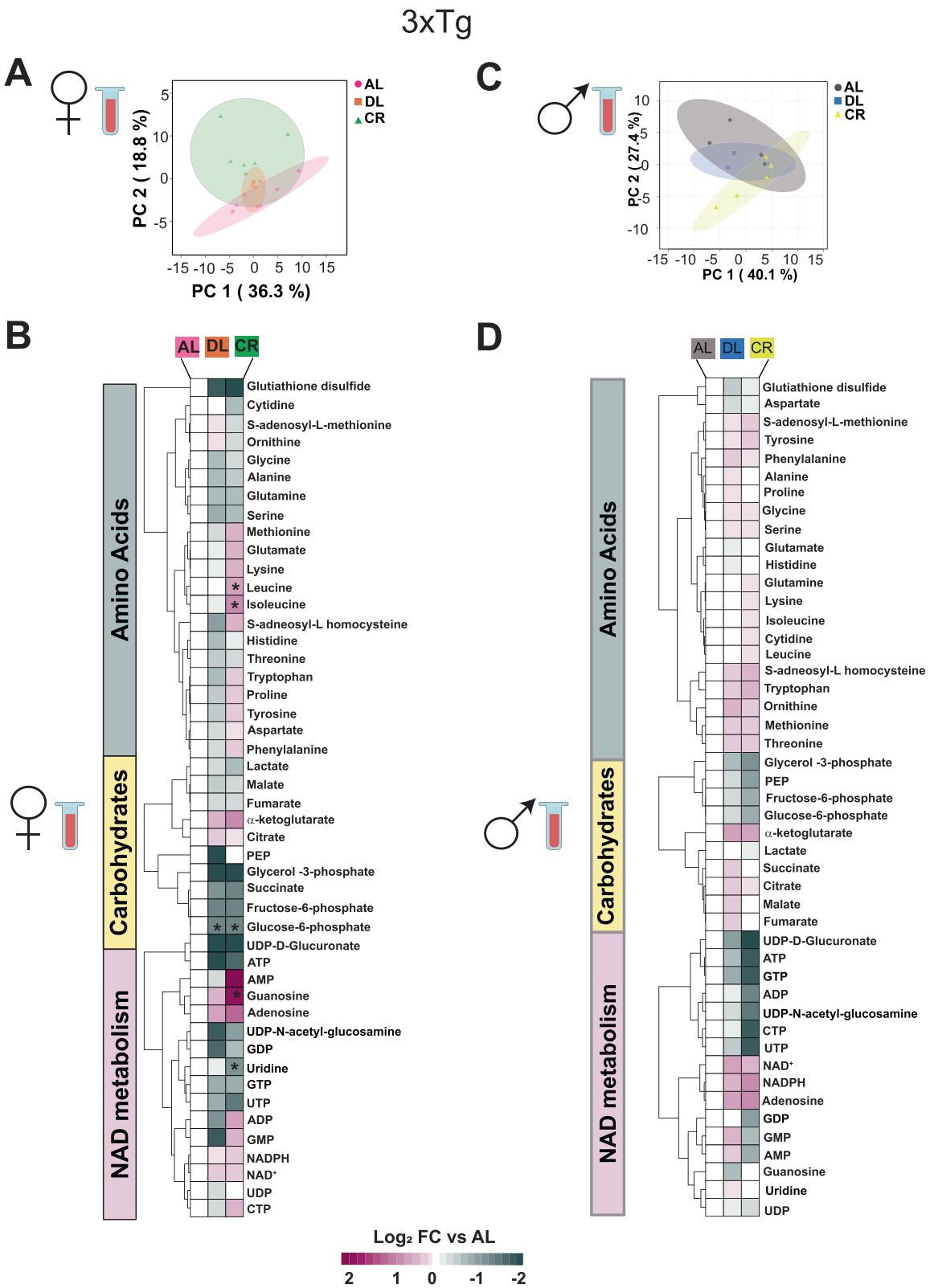

Fig. 4 | Plasma metabolome displays sex specific effects of fasting and energy restriction in 3xTg-AD mice. Targeted metabolomics were performed on the plasma of female and male 3xTg mice fed *ad libitum* (AL), Diluted AL (DL) or Caloric Restricted (CR with fasting between once-daily meals) diets. Principal Component Analysis (PCA) of plasma metabolites from 3xTg females (**A**) and males (**C**) fed on an AL, DL or CR diets. Heatmap of 47 targeted metabolites, represented as log2-fold change vs. AL-fed mice in females (**B**) and males. (**D**). **B** *p < 0.05 vs. AL-fed mice, two-tailed Tukey's test post ANOVA. **A**–**D** For females n = 5 AL, n = 6 DL, n = 6 CR biologically independent mice per group were used. For males n = 4 AL, n = 3 DL, n = 5 biologically independent mice per group were used. Source data are provided as a Source Data file.

https://doi.org/10.1038/s41467-025-62416-3

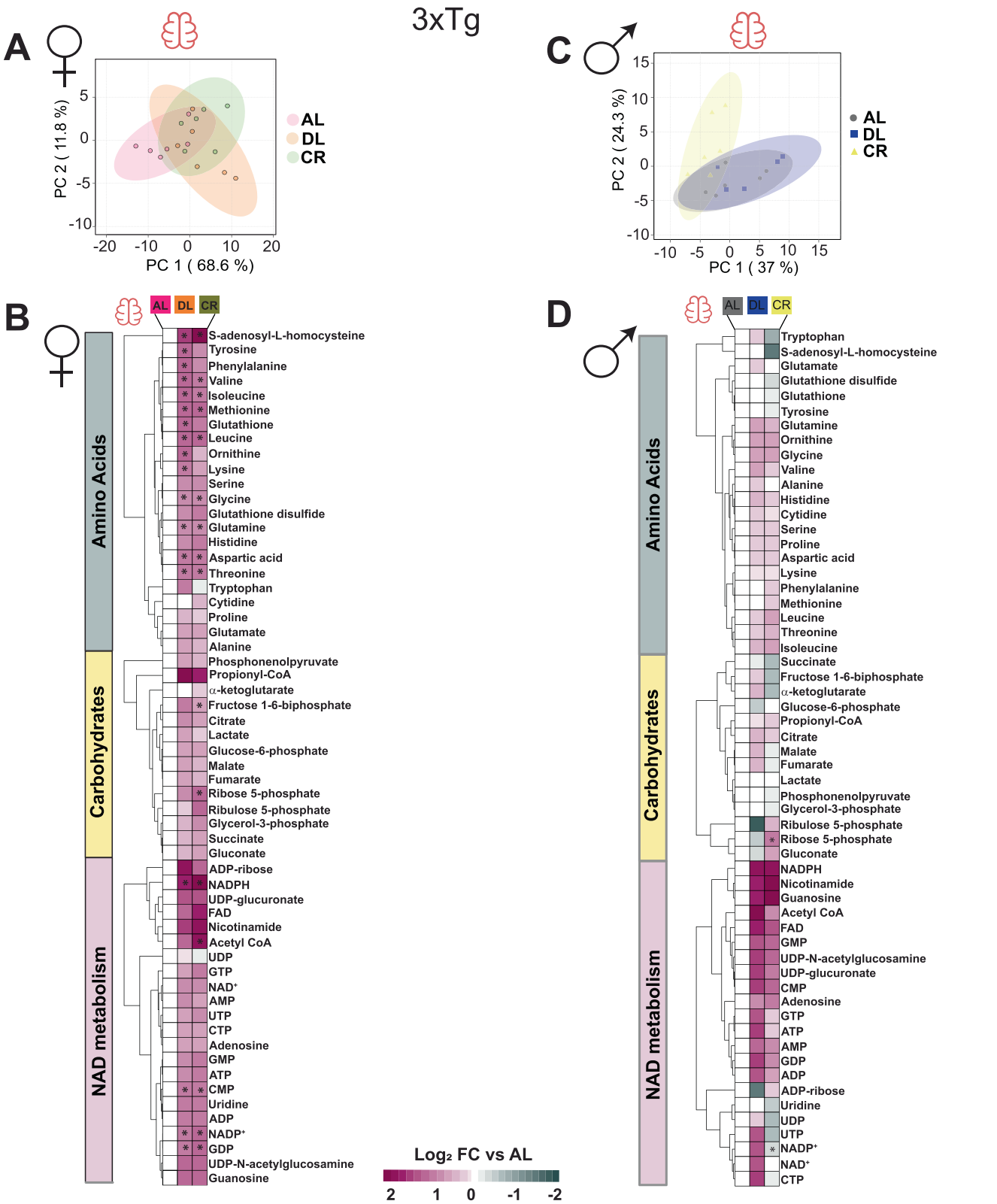

Fig. 5 | Overlapping brain metabolome profile in female 3xTg-AD mice under energy restriction and once-per-day CR regimen. Targeted metabolomics were performed on the brain of female and male 3xTg mice fed *ad libitum* (AL), Diluted AL (DL) or Caloric Restricted (CR with fasting between once-daily meals) diets. Principal Component Analysis (PCA) of plasma metabolites from 3xTg females (**A**) and males (**C**) fed on an AL, DL or CR diets. (**B**, **D**) Heatmap of 47 targeted metabolites, represented as log2-fold change vs. AL-fed mice in females (**B**) and males (**D**). **B**, **D** *$p < 0.05$ vs. AL-fed mice, two-tailed Tukey's test post one-way ANOVA. **A**–**D** For females n = 6 biologically independent mice per group were used. For males n = 6 AL, n = 5 DL, n = 6 biologically independent mice per group were used. Source data are provided as a Source Data file.

https://doi.org/10.1038/s41467-025-62416-3

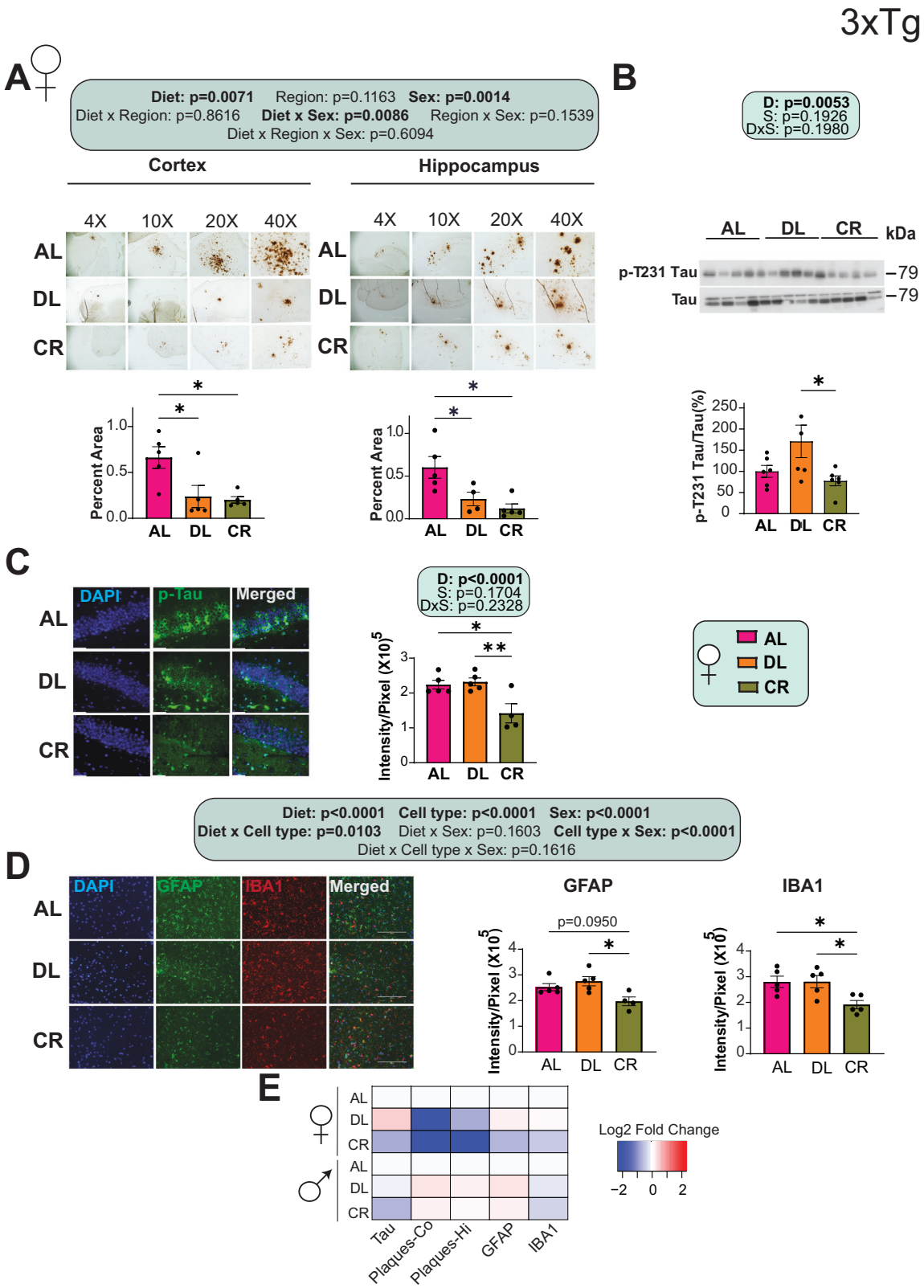

As expected with CR, both males and females had reduced mTORC1 signaling and autophagy activation. However, females displayed significant reduction in mTORC1 when compared to DL-fed mice, whereas males showed significant reduction when compared to AL-fed mice. The extent of autophagy activation by CR was similar in both sexes, though induction of BDNF by CR was more pronounced in males following energy restriction.

These sex differences were even more clearly seen in our metabolomic analysis of plasma and brain tissue in the 3xTg mice. We observed significant changes in metabolic pathways in response to diet in females, with some overlap in the response to DL and CR feeding, while males showed many fewer changes with no overlapping changes between the DL and CR groups. One key pathway identified in females across both plasma and brain tissues was the cysteine and methionine

Fig. 6 | Fasting required for mitigating hyperphosphorylation of tau, but not Aβ plaques in female 3xTg-AD mice. A–C Analysis of AD neuropathology in female 3xTg mice fed on *ad libitum* (AL), Diluted AL (DL) or Caloric Restricted (CR with fasting between once-daily meals). **A** Representative plaque images in the cortex and hippocampus of female 3xTg mice. scale bar in the 4x image is 1000 μM, 10x image is 400 μM, 20x is 200 μM and 40x is 100 μM. Quantification of plaque area in female cortex n = 5 biologically independent mice per group and for hippocampus n = 5 AL, n = 4 DL and n = 5 CR fed 3xTg biologically independent mice. **B** Western blot analysis of phosphorylated Thr231 Tau in female(n = 6 biologically independent mice/group). **C** Representative immunofluorescence images of 3xTg females stained with p-Tau Thr231 antibody (AT180), 63x magnification shown; scale bar 50 μM. Quantitative analysis of fluorescence intensity. n = 5 AL, n = 5 DL, n = 4 CR fed 3xTg biologically independent mice. **D** Immunostaining and quantification for astrocytes (GFAP) and microglia (IBA1) in female 3xTg mice. 20x magnification shown; Scale bar 200 μM. n = 5 AL, n = 5 DL, n = 4 CR for GFAP and n = 5 biologically independent mice/group for IBA1. **E** Heat map representation of the neuropathological findings in female and male 3xTg mice; log_2 fold-change relative to AL-fed mice of each sex. **A** Statistics for the overall effects of diet, sex, region, and their interactions represent the p values from a three-way ANOVA; *p < 0.05, from a two-tailed Tukey's test post ANOVA. **B**, **C** Statistics for the overall effects of diet (D), sex (S) and their interaction (DxS) represent the p values from a 2-way ANOVA; *p < 0.05, from a two-tailed Tukey's test post ANOVA. **C** AL vs CR $*p = 0.0162$, DL vs CR $*p = 0.0093$. (**D**) Statistics for the overall effects of diet, sex, and cell type (GFAP or IBA1 stain) represent the p values from a three-way ANOVA; *p < 0.05, two-tailed Tukey's test post ANOVA. GFAP; DL vs CR $*p = 0.0182$. IBA1; AL vs CR $*p = 0.0286$, DL vs CR $*p = 0.0274$. AL; *ad libitum*, DL; Diluted AL, CR; Caloric Restricted. Data represented as mean ± SEM. Source data are provided as a Source Data file.

metabolism pathway. This is particularly interesting given that methionine restriction has been previously shown to improve metabolic outcomes as well as improve longevity in animal models[71–73]. Furthermore, components of the circulating methionine cycle are known to play an important role in the pathogenesis of AD[74,75]. Methionine is a key regulator of DNA and histone methylation[76–79], and methionine cycle disruptions have been linked to altered DNA methylation patterns in AD, which affects neuroinflammation[80–82]. Thus, the role of methionine metabolism and its epigenetic effects on the development and progression of AD will be an important area for further study.

Interestingly, we found a significant overlap in metabolite abundance between the DL and CR groups in the brains of female 3xTg mice. These overlapping metabolites were primarily amino acids, which were increased in both DL and CR groups compared to control mice. Consistent with previous studies in mice, we also observed an increase in branched-chain amino acids (Leucine, Isoleucine, and Valine) in the brains of both DL and CR-fed female mice[12,83].

The current study has several limitations that need to be addressed in future research. One significant limitation is the use of a diet diluted with indigestible cellulose (DL); while potentially a low-energy diet could be deleterious for a variety of reasons, in wild-type mice energy restriction induced by a low energy diet has similar impacts on lifespan as energy restriction induced by many feeding small meals of a normal diet[54]. In our previous work, we found that a DL diet does not impair macronutrient absorption or gut integrity; however, the effects of DL on the gut microbiome or micronutrient absorption remains an open question. Future studies should examine these potentially confounding factors.

In this study, we used intraperitoneally administered glucose to assess glucose metabolism. While this is an established technique[84,85], this approach is less physiologically relevant than orally administered glucose, as it bypasses incretin hormone signaling that could significantly impact insulin secretion and glucose homeostasis[86]. Future studies should consider the use of orally administered glucose to provide a more physiologically relevant assessment of differences in glucose metabolism.

We also did not study the effects of fasting alone, without energy restriction, on AD pathology and cognition in 3xTg mice. Based on the results we and others have observed in wild-type mice[12,55], we hypothesize that fasting may be sufficient to recapitulate many of the benefits of CR on cognition and AD pathology, but this has not been tested. Additionally, while there are many benefits of using the 3xTg mouse model of AD[87], the use of other AD mouse models could provide additional insight, particularly into whether the benefits of CR are mediated via its remediations of tauopathy.

Our molecular analyses were limited; while we examined the effects of mTOR signaling and autophagy, we did not take a broader and unbiased view of the molecular pathways engaged by CR; fasting and energy restriction likely impinge on many other pathways which have been shown to impact AD pathology, e.g., AMPK and SIRT1[88–90]. Our molecular analysis did not explore the transcriptome or the proteome and was limited to the whole brain and plasma, rather than narrowing in on specific brain regions. A growing body of literature suggests other tissues outside the brain, including the liver, can also influence the development and progression of AD[91–93]. Lastly, our study focused exclusively on the brain and plasma. Given the significant results we observed in insulin sensitivity and the overlap in metabolites in the brain, it would be important to include analyses of the liver, skeletal muscle, and adipose tissue in future studies. These tissues are key contributors to metabolic health, and examining their responses could provide important insights into the systemic effects of CR and fasting in AD mice.

In conclusion, our findings strongly suggest that while not all benefits of CR require fasting, fasting plays a critical role in CR-induced improvements in AD pathology. Although energy restriction alone was sufficient to mitigate plaque pathology in 3xTg females and improve certain aspects of cognition, fasting was essential for the reduction of tau pathology as well as many other molecular and histological markers of AD and the full cognitive benefits of CR. Our results suggest that CR with fasting – or, potentially, although we have not tested it here, fasting alone – could be a promising therapeutic approach to AD. Even if this diet regiment is too arduous for many or for the elderly in particular our results suggest that potential CR mimetic agents should aim to mimic the results of daily fasting, and not simply energy restriction, to fully capture the benefits of CR for AD.

Methods

Animals

All procedures were performed in accordance with institutional guidelines and were approved by the Institutional Animal Care and Use Committee (IACUC) of the William S. Middleton Memorial Veterans Hospital and the University of Wisconsin-Madison IACUC (Madison, WI, USA). Male and female homozygous 3xTg-AD mice and their non-transgenic littermates were obtained from The Jackson Laboratory (Bar Harbor, ME, USA) and were bred and maintained at the vivarium with food and water available *ad libitum*. Prior to the start of the experiments at 6 months they were randomly assigned to different groups based on their body weight and diet. Mice were acclimatized on a 2018 Teklad Global 18% Protein Rodent Diet for 1 week before randomization and were singly housed. All mice were maintained at a temperature of approximately 22 °C, and health checks were completed on all mice daily.

At the start of the experiment, mice were randomized to three different groups (1) AL, *ad libitum* diet; (2) DL, Diluted *ad libitum* diet where animals were provided with *ad libitum* access to a low-energy diet diluted with indigestible cellulose, which reduced caloric intake by ~30% and (3) CR, animals in which calories were restricted by 30%, and animals were fed once per day during the start of the light period; Animals fed the AL and CR diet were fed 2018 Teklad Global 18% Protein Rodent Diet (Envigo) and animals fed a DL diet were fed Teklad 2018 with 50%

https://doi.org/10.1038/s41467-025-62416-3

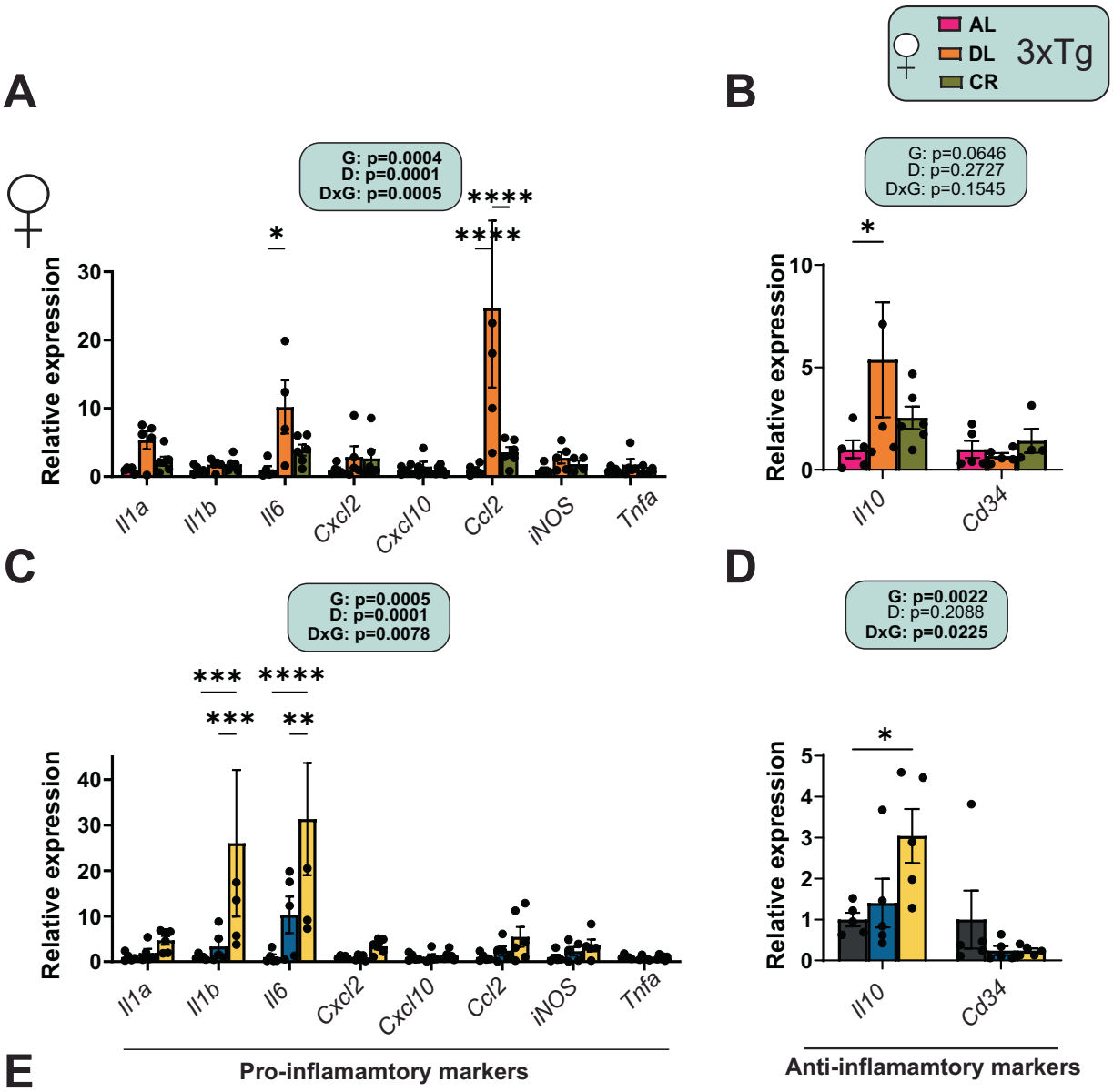

Summary of Two-way ANOVA (Diet x Sex)

Genes	Diet (p)	Sex (p)	Diet x Sex (p)
Il1a	**0.0068**	0.6211	**0.0051**
Il1b	0.1025	0.1110	0.1194
Il16	**0.0174**	0.0521	**0.0244**
Cxcl2	0.0963	0.5505	0.2942
Cxcl10	0.8527	0.9975	0.6386
Ccl2	**0.0361**	0.0808	**0.0261**
iNOS	0.1003	0.5244	0.4045
Tnfa	0.7221	0.2207	0.3345
Il10	0.1469	0.2520	0.1503
Cd34	0.3918	0.1212	0.3713

Fig. 7 | Diet induced differential expression of neuroinflammatory genes in 3xTg-AD mice. A–**D** Expression of the indicated pro-inflammatory and anti-inflammatory genes from female (**A**, **B**) and male (**C**, **D**) 3xTg mice fed on *ad libitum* (AL), Diluted AL (DL) or Caloric Restricted (CR with fasting between once-daily meals) diets from 6–15 months of age using qPCR. **E** Summary of statistical outcomes from two-way ANOVAs (Diet x Sex) conducted separately for each gene. **A**, **B** n = 5 AL, n = 5 DL, n = 6 CR fed 3xTg biologically independent female mice (**C**, **D**) n = 5 AL, n = 5 DL, n = 5 CR fed 3xTg biologically independent male mice. **A**–**D** Statistics for the overall effect of diet (D), genes (G), and the interaction represent the p values from a two-way ANOVA; *p < 0.05, **p < 0.01, ***p < 0.001, ****p < 0.0001, two-tailed Sidak's post-test examining the effect of parameters identified as significant in the two-way ANOVA. **E** Statistics for the overall effect of diet (D), sex (S), and the interaction represent the p values from a two-way ANOVA. Data represented as mean ± SEM. Source data are provided as a Source Data file.

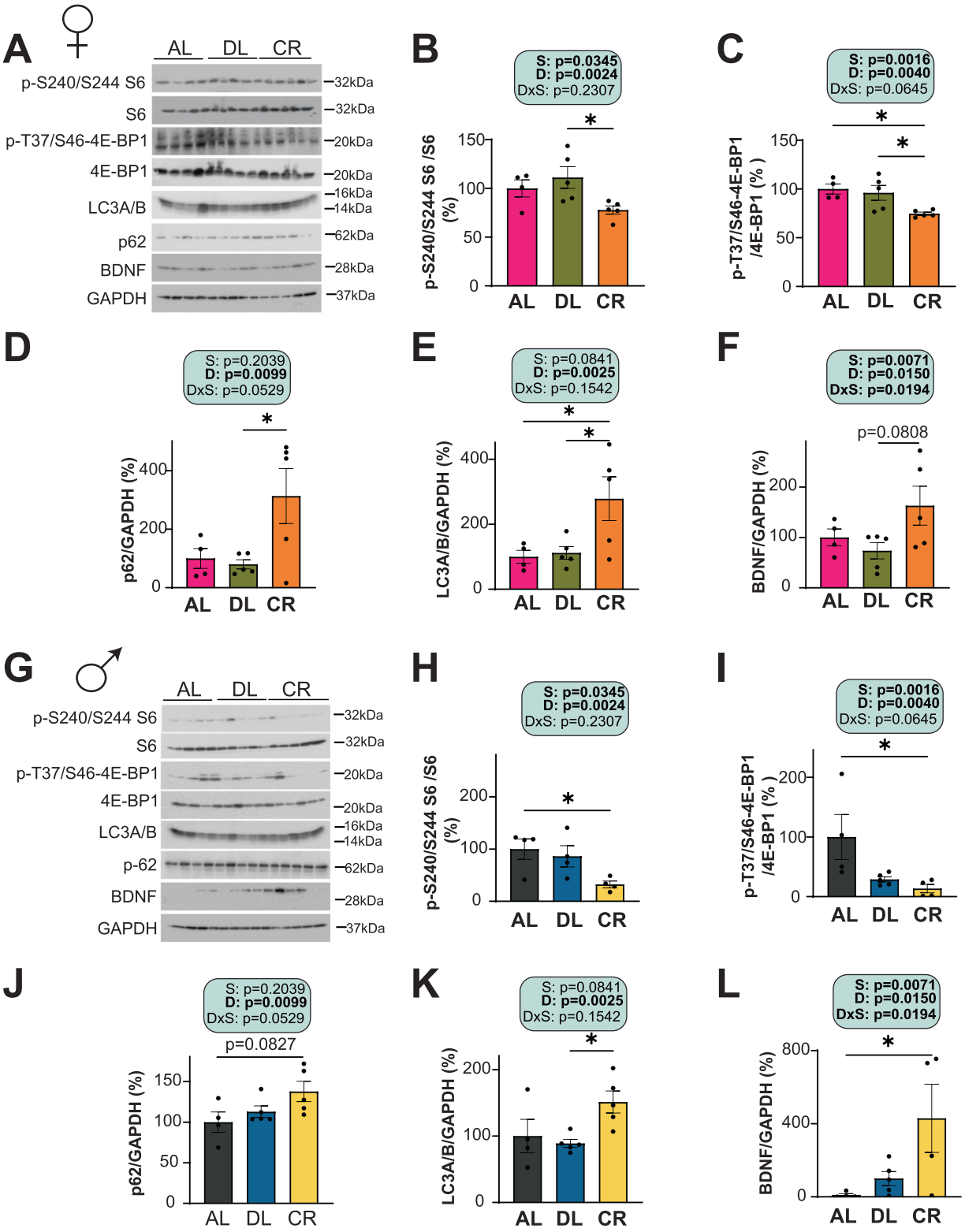

cellulose (TD.170950). Diet descriptions, compositions and item numbers are provided in Supplementary Data 1. This manuscript abides by the ARRIVE guidelines for the reporting of animal experiments.

In vivo procedures

Glucose and Insulin tolerance tests were performed by fasting the mice overnight and then injecting either glucose (1 g kg^{-1}) or insulin (0.75 U kg^{-1}), respectively, intraperitoneally[73,84]. We timed the assays in such a way that all the groups were fasted for similar durations of time to minimize confounding factors affecting the tests. Specifically, after 3 hours of feeding the CR mice at the start of the light cycle, all the dietary groups were fasted overnight (~ 21-22 hours) before performing the tolerance tests the following morning. Glucose measurements were taken using a Bayer Contour blood glucose meter (Bayer,

Fig. 8 | Differential effects of feeding regimens on brain mTORC1 signaling and autophagy activation in 3xTg mice. A–L The phosphorylation of S6 and 4E-BP1, and the expression of p62, LC3A/B and BDNF was assessed by western blotting of whole brain lysates of 3xTg mice fed on *ad libitum* (AL), Diluted AL (DL) or Caloric Restricted (CR with fasting between once-daily meals) diets from 6-15 months. Quantification of the phosphorylation of p-S240/S244 S6 (**B**) and T37/S46 4E-BP1 (**C**), relative to expression of S6 and 4E-BP1, respectively in females. Quantification of p62 expression (**D**) LC3A/B expression (**E**) and BDNF expression (**F**) relative to expression of GAPDH in females. Quantification of the phosphorylation of p-S240/S244 S6 (**H**) and T37/S46 4E-BP1 (**I**), relative to expression of S6 and 4E-BP1, respectively, in males. Quantification of p62 expression (**J**), LC3A/B expression (**K**), and BDNF expression (**L**) relative to expression of GAPDH in males. (**B**–**F**) n = 4 AL, n = 5 DL and n = 5 CR fed 3xTg biologically independent female mice. **H** n = 4 AL, n = 4 DL and n = 4 CR (**I**) n = 4 AL, n = 5 DL and n = 4 CR (**J**, **K**) n = 4 AL, n = 5 DL and n = 5 CR (**L**) n = 4 AL, n = 5 DL and n = 4 CR fed 3xTg biologically independent male mice. **B**–**F**, **H**–**L** Statistics for the overall effects of diet (D), sex (S) and their interaction (DxS) represent the p values from a 2-way ANOVA; *p < 0.05, from a two-tailed Tukey's test post ANOVA. Data represented as mean ± SEM. BDNF; Brain derived neurotrophic factor. Source data are provided as a Source Data file.

Leverkusen, Germany) and test strips. Mouse body composition was determined using an EchoMRI Body Composition Analyzer (EchoMRI, Houston, TX, USA). For determining metabolic parameters [O2, CO2, food consumption, respiratory exchange ratio (RER), energy expenditure] and activity tracking, the mice were acclimated to housing in an Oxymax/CLAMS-HC metabolic chamber system (Columbus Instruments) for ~24 h and data from a continuous 24 h period was then recorded and analyzed. Following 3 hours of feeding the CR mice at the start of the light cycle, all dietary groups underwent a 3 hr fast, followed by cervical dislocation and tissues for molecular analysis were flash-frozen in liquid nitrogen or fixed and prepared as described in the methods below.

Behavioral assays

All mice underwent behavioral phenotyping when they were twelve months old. The Novel Object Recognition test (NOR) was performed in an open field where the movements of the mouse were recorded via a camera that is mounted above the field. Before each test mice were acclimatized in the behavioral room for 30 minutes and were given a 5 min habituation trial with no objects on the field. This was followed by test phases that consisted of two trials that are 24 hrs apart: Short Term Memory test (STM) and Long Term Memory test (LTM). In the first trial, the mice were allowed to explore two identical objects placed diagonally on opposite corners of the field for 5 minutes. Following an hour after the acquisition phase, STM was performed and 24 hrs later, LTM was done by replacing one of the identical objects with a novel object. The results were quantified using a discrimination index (DI), representing the duration of exploration for the novel object compared to the old object.

For Barnes maze, the test involves 3 phases: habituation, acquisition training and the memory test. During habituation, mice were placed in the arena and allowed to freely explore the escape hole, escape box, and the adjacent area for 2 min. Following that during acquisition training the mice were given 180 s to find the escape hole, and if they failed to enter the escape box within that time, they were led to the escape hole. After 4 days of training, on the 5th day (STM) and 12th day (LTM) the mice were given 90 s memory probe trials. The latency to enter the escape hole, distance traveled, and average speed were analyzed using Ethovision XT (Noldus).

Immunoblotting

Tissue samples from brain were lysed in cold RIPA buffer supplemented with phosphatase inhibitor and protease inhibitor cocktail (Thermo Fisher Scientific, Waltham, MA, USA) using a FastPrep 24 (M.P. Biomedicals, Santa Ana, CA, USA) with bead-beating tubes (16466–042) from (VWR, Radnor, PA, USA) and zirconium ceramic oxide bulk beads (15340159) from (Thermo Fisher Scientific, Waltham, MA, USA). Protein lysates were then centrifuged at 13,300 rpm for 10 min and the supernatant was collected. Protein concentration was determined by Bradford (Pierce Biotechnology, Waltham, MA, USA). 20 µg protein was separated by SDS–PAGE (sodium dodecyl sulfate–polyacrylamide gel electrophoresis) on 8%, 10%, or 16% resolving gels (ThermoFisher Scientific, Waltham, MA, USA) and transferred to PVDF membrane (EMD Millipore, Burlington, MA, USA). The phosphorylation status of mTORC1 substrates including S6 S240/S244 and 4E-BP1 T37/S46 were assessed in the brain along with autophagy receptor p62 (sequestosome 1, SQSTM1) and the autophagosome marker LC3A/B. Tau pathology was assessed by western blot with anti-tau antibody. Antibody vendors, catalog numbers and the dilution used are provided in Supplementary Data 13. Imaging was performed using a Bio-Rad Chemidoc MP imaging station (Bio-Rad, Hercules, CA, USA). Quantification was performed by densitometry using NIH ImageJ software.

Histology for AD neuropathology markers

Following cervical dislocation, the brains were collected and divided into two hemispheres. The right hemisphere was fixed in formalin for histology while the left hemisphere was snap frozen for molecular analysis. For amyloid plaque staining, briefly brain sections were deparaffinized and rehydrated according to standard protocol. For epitope retrieval, mounted slides were pretreated in 70% formic acid at room temperature for 10 min. Tissue sections were subsequently blocked with normal goat serum (NGS) at room temperature for 1 hr, then incubated with monoclonal antibodies 6E10 (1:100), at 4 °C overnight. Aβ immunostained profiles were visualized using diaminobenzidine chromagen. For p-Tau staining and glial activation, brains were analyzed with anti-GFAP (astrocytic marker), and anti-Iba1 (microglial marker) antibodies, respectively. The following primary antibodies were used: phospho-Tau (Thr231) monoclonal antibody (AT180) (Thermo Fisher Scientific; # MN1040, 1:100) anti-GFAP (Thermo Fisher; # PIMA512023; 1:1,000), anti-IBA1 (Abcam; #ab178847; 1:1,000). Sections for plaque and glia staining were imaged using an EVOS microscope (Thermo Fisher Scientific Inc., Waltham, MA, USA) at a magnification of 4X, 10X and 40X magnification. Sections for tau staining were imaged using Leica DMI6000B Inverted microscope at a magnification of 63x. Image-J was used for quantification by converting images into binary images via an intensity threshold and positive area was quantified[94].

Quantitative real-time PCR. RNA was extracted from whole brain using TRI Reagent and PureLink mini-RNA kit (Thermo Fisher Scientific, Cat # 12183020) according to the manufacturer's protocol (Thermo Fisher Scientific). The concentration and purity of RNA were determined by absorbance at 260/280 nm using Nanodrop (Thermo Fisher Scientific). 1 µg of RNA was used to generate cDNA (Superscript III; Invitrogen, Carlsbad, CA, USA). Oligo dT primers and primers for real-time PCR were obtained from Integrated DNA Technologies (IDT, Coralville, IA, USA); Primer sequences are in Supplementary Data 14. Reactions were run on an StepOne Plus machine (Applied Biosystems, Foster City, CA, USA) with Sybr Green PCR Master Mix (Invitrogen). Actin was used to normalize the results from gene-specific reactions.

Targeted Metabolomics on Plasma

Metabolite extraction. Plasma (20µL from 29 female and male samples) was transferred to an individual 1.5 mL microcentrifuge tube and incubated with 400µL −80 °C 80:20 Methanol (MeOH): H2O extraction solvent on dry ice for 5 minutes post-vortexing. Serum homogenate was centrifuged at 21,000 × *g* for 5 minutes at 4 °C. Supernatant

https://doi.org/10.1038/s41467-025-62416-3

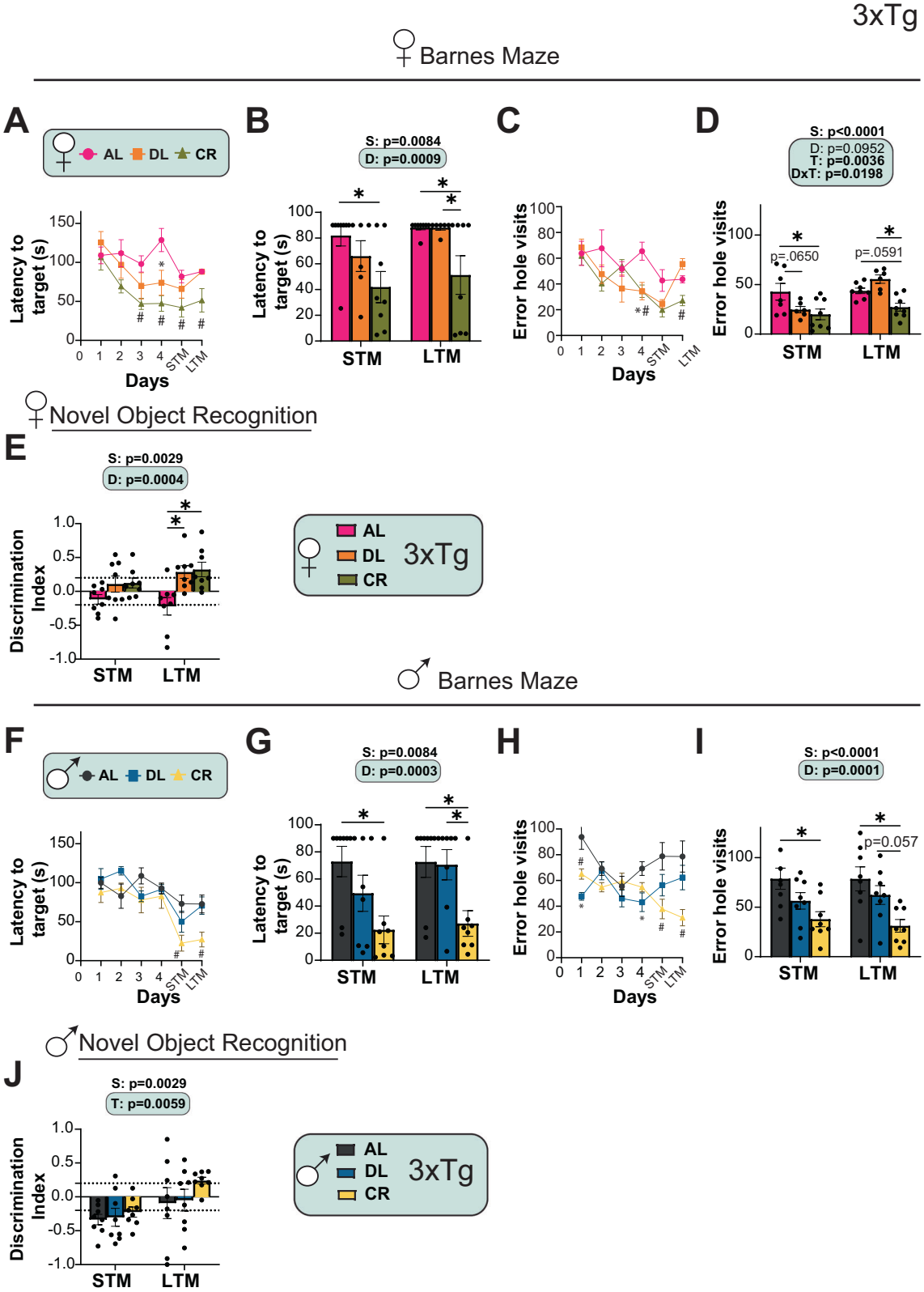

was transferred to 1.5 mL microcentrifuge tube after which the remining pellet was resuspended in 400 µL −20 °C 40:40:20 Acetonitrile (ACN): MeOH: H2O extraction solvent and incubated on ice for 5 minutes. Serum homogenate was again centrifuged at 21,000 × *g* for 5 minutes at 4 °C after which the supernatant was pooled with the previously isolated metabolite fraction. The 40:20:20 ACN: MeOH:H_2O extraction was then repeated. Next, the pooled metabolite extract for each sample was transferred to a 1.5 mL microcentrifuge Eppendorf tube and completely dried using a Thermo Fisher Savant ISS110 SpeedVac. Dried metabolite extracts were resuspended in 100 µL of LCMS-graded water following microcentrifugation for 5 minutes at 21,000 xg at 4 C to pellet any remaining insoluble debris. Supernatant was then transferred to a glass vial for LC-MS analysis.

Fig. 9 | Fasting required for spatial memory recognition in both sexes of 3xTg mice. A–J Behavioral phenotyping after 3xTg mice were on *ad libitum* (AL), Diluted AL (DL) or Caloric Restricted (CR with fasting between once-daily meals) diets for 6 months. Latency of target in Barnes Maze during training (**A**) and in short term memory (STM) and long-term memory (LTM) tests by female mice (**B**). Error hole visits during training (**C**) in STM and LTM tests by female mice (**D**). **E** STM and LTM tests from NOR assay (**A**–**E**) n = 8 AL, n = 6 DL and n = 8 CR fed 3xTg biologically independent female mice. Latency of target in Barnes Maze during training (**F**) and in STM and LTM tests by male mice (**G**). Error hole visits during training (**H**) in STM and LTM tests by male mice (**I**). **J** STM and LTM tests from NOR assay (**F**–**J**) n = 8 AL, n = 8 DL and n = 8 CR fed 3xTg biologically independent male mice. **A**, **C**, **F**, **H** Two-way RM ANOVA followed by Dunnett's test vs. AL; *p < 0.05 AL vs DL, # p < 0.05 AL vs CR. **B**, **D**, **E**, **G**, **I**, **J** Statistics for the overall effect of diet (D), time (T) and the interaction (DxT) represent the p value from a two-way ANOVA; *p < 0.05 from a two-tailed Sidak's post-test examining the effect of parameters identified as significant in the two-way ANOVA. The overall effect of sex (S) represents the p-value from a separately completed three-way ANOVA. **A** AL vs CR #$p = 0.0030$ (day 3), AL vs DL *$p = 0.0462$, AL vs CR #$p = 0.0013$ (day 4), AL vs CR #$p = 0.0320$ (STM), AL vs CR #$p = 0.0424$ (LTM). **C** AL vs DL *$p = 0.0126$, AL vs CR #$p = 0.058$ (day 4), AL vs CR #$p = 0.0097$ (LTM). **D** STM; AL vs CR *$p = 0.0074$, LTM; DL vs CR *$p = 0.0013$. **F** AL vs CR #$p = 0.0094$ (STM), AL vs CR #$p = 0.0160$ (LTM) (H) AL vs DL *$p = 0.0030$, AL vs CR #$p = 0.0383$ (day 1), AL vs DL *$p = 0.0227$ (day 4), AL vs CR #$p = 0.0157$ (STM), AL vs CR #$p = 0.0102$ (LTM). **I** STM; AL vs CR *$p = 0.0102$, LTM; AL vs CR *$p = 0.00024$. Data represented as mean ± SEM. NOR: Novel Object Recognition, BM: Barnes Maze. Source data are provided as a Source Data file.

Targeted metabolomics on brain

Metabolite Extraction. Following cervical dislocation, the brains were collected and divided into two hemispheres. The right hemisphere was fixed in formalin for histology while the left hemisphere was immediately snap-frozen in liquid nitrogen before being evenly pulverized. This procedure was performed consistently across all animals to minimize variability. Approximately 10 mg of tissue from 30 female and male brains were homogenized on ice using a dounce homogenizer in 400 μL of 80:20 methanol. The homogenate was then transferred to a 1.5 mL microcentrifuge tube. An additional 100 μL of the solvent was used to rinse the mortar and was subsequently added to the same tube. The mixture was incubated on ice for 5 minutes before being centrifuged at 21,000 × *g* for 5 minutes at 4 °C. After centrifugation, 500 μL of the supernatant was transferred to a fresh 1.5 mL microcentrifuge tube and dried completely using a Thermo Fisher Savant ISS110 SpeedVac. The protein pellet was resuspended in 100 μL RIPA buffer (10 mM Tris-HCl, pH 8.0, 1 mM EDTA, 0.5 mM EGTA, 1% Triton X-100, 0.1% Sodium Deoxycholate, 0.1% SDS, and 140 mM NaCl) to normalize the intensity values for each targeted metabolite. The dried metabolite extracts were resuspended in 100 L of LC-MS-grade water and centrifuged again at 21,000 × *g* for 5 minutes at 4 °C to pellet any remaining insoluble debris. The resulting supernatant was then transferred to a glass vial for LCMS analysis.

LC-MS metabolite analysis. Each prepared metabolite sample was injected onto a Thermo Fisher Scientific Vanquish UHPLC with a Waters Acquity UPLC BEH C18 column (1.7 μm, 2.1 × 100mm; Waters Corp., Milford, MA, USA) and analyzed using a Thermo Fisher Q Exactive orbitrap mass spectrometer in negative ionization mode. LC separation was performed over a 25 minute method with a 14.5 minute linear gradient of mobile phase (buffer A, 97% water with 3% methanol, 10 mM tributylamine, and acetic acid-adjusted pH of 8.3) and organic phase (buffer B, 100% methanol) (0 minute, 5% B; 2.5 minute, 5% B; 17 minute, 95% B; 19.5 minute, 5% B; 20 minute, 5% B; 25 minute, 5% B, flow rate 0.2 mL/min). A quantity of 10 μL of each sample was injected into the system for analysis. The ESI settings were 30/10/1 for sheath/aux/sweep gas flow rates, 2.50 kV for spray voltage, 50 for S-lens RF level, 350 C for capillary temperature, and 300 C for auxiliary gas heater temperature. MS1 scans were operated at resolution = 70,000, scan range = 85–1250 m/z, automatic gain control target = 1 × 106, and 100 ms maximum IT. Metabolites were identified and quantified using El-MAVEN (v0.12.1-beta) with metabolite retention times empirically determined in-house. Peak Area top values were imported into MetaboAnalyst for statistical analysis (one factor) using default settings.

Metabolomics analysis. Metabolomics data was analyzed using MetaboAnalyst 6.0[95] using Single Factor Analysis with recommended settings. Data was filtered by interquartile range, median normalized and auto scaled. Fold changes were calculated relative to the AL group and $\log_2$ transformed subsequently for visualization in the heatmap. $\log_2$ fold-changes and associated uncorrected and corrected p-values can be found in Supplementary Data 4, 9 and 12. For individual metabolites, one-way ANOVA followed by Tukey's multiple comparisons post hoc test was performed using GraphPad Prism 9.0. Metabolites were considered significant at $p < 0.05$ (unadjusted) for pathway enrichment analysis. PCA plots and pathway enrichment analyses were performed using significantly altered metabolites in MetaboAnalyst 6.0. Heatmaps and pathway dot plots were generated using R (version 3.3.1).

Statistical analysis. All statistical analyses were conducted using Prism, version 9 (GraphPad Software Inc., San Diego, CA, USA). Tests involving multiple factors were analyzed using either a three-way analysis of variance (ANOVA) with diet, time, and sex as variables, a two-way ANOVA with diet and time as variables, followed by Sidak's post hoc test, a two-way repeated measures (RM) ANOVA for longitudinal data, followed by Dunnett's post hoc test or by one-way ANOVA followed by Tukey's post hoc test as specified in the figure legends. Metabolomics data were analyzed using metaboanalyst (version 6.0). Kaplan–Meir survival analysis of 3xTg mice was performed with log-rank comparisons. Data are presented as the mean ± SEM unless otherwise specified.

Reporting summary

Further information on research design is available in the Nature Portfolio Reporting Summary linked to this article.

Data availability

Source data are provided with this paper. Targeted brain metabolomics data has been deposited in MassIVE with accession code MSV000095847 [https://doi.org/10.25345/C5N873B30]. Targeted plasma metabolomics data has been deposited in MassIVE with accession code MSV000095887 [https://doi.org/10.25345/C5GF0N767]. Source data are provided with this paper.

References

1. Rajan, K. B. et al. Population estimate of people with clinical Alzheimer's disease and mild cognitive impairment in the United States (2020-2060). *Alzheimers Dement.* **17**, 1966–1975 (2021).
2. Alzheimer's Association. Alzheimer's disease facts and figures. *Alzheimers Dement.* **19**, 1598–1695 (2023).
3. Green, C. L., Lamming, D. W. & Fontana, L. Molecular mechanisms of dietary restriction promoting health and longevity. *Nat. Rev. Mol. Cell Biol.* **23**, 56–73 (2022).
4. Halagappa, V. K. et al. Intermittent fasting and caloric restriction ameliorate age-related behavioral deficits in the triple-transgenic mouse model of Alzheimer's disease. *Neurobiol. Dis.* **26**, 212–220 (2007).
5. Mouton, P. R., Chachich, M. E., Quigley, C., Spangler, E. & Ingram, D. K. Caloric restriction attenuates amyloid deposition in middle-aged dtg APP/PS1 mice. *Neurosci. Lett.* **464**, 184–187 (2009).

6. Schafer, M. J. et al. Reduction of beta-amyloid and gamma-secretase by calorie restriction in female Tg2576 mice. *Neurobiol. Aging* **36**, 1293–1302 (2015).
7. Wang, J. et al. Caloric restriction attenuates beta-amyloid neuropathology in a mouse model of Alzheimer's disease. *FASEB J.* **19**, 659–661 (2005).
8. Qin, W. et al. Calorie restriction attenuates Alzheimer's disease type brain amyloidosis in Squirrel monkeys (Saimiri sciureus). *J. Alzheimer's Dis.* **10**, 417–422 (2006).
9. Witte, A. V., Fobker, M., Gellner, R., Knecht, S. & Floel, A. Caloric restriction improves memory in elderly humans. *Proc. Natl. Acad. Sci. USA* **106**, 1255–1260 (2009).
10. Acosta-Rodriguez, V. A., de Groot, M. H. M., Rijo-Ferreira, F., Green, C. B. & Takahashi, J. S. Mice under caloric restriction self-impose a temporal restriction of food intake as revealed by an automated feeder system. *Cell Metab.* **26**, 267–277.e262 (2017).
11. Wahl, D. et al. Cognitive and behavioral evaluation of nutritional interventions in rodent models of brain aging and dementia. *Clin. Inter. Aging* **12**, 1419–1428 (2017).
12. Pak, H. H. et al. Fasting drives the metabolic, molecular and geroprotective effects of a calorie-restricted diet in mice. *Nat. Metab.* **3**, 1327–1341 (2021).
13. Oddo, S. et al. Triple-transgenic model of Alzheimer's disease with plaques and tangles: intracellular Abeta and synaptic dysfunction. *Neuron* **39**, 409–421 (2003).
14. Bruss, M. D., Khambatta, C. F., Ruby, M. A., Aggarwal, I. & Hellerstein, M. K. Calorie restriction increases fatty acid synthesis and whole body fat oxidation rates. *Am. J. Physiol. Endocrinol. Metab.* **298**, E108–E116 (2010).
15. Ansoleaga, B. et al. Deregulation of purine metabolism in Alzheimer's disease. *Neurobiol. Aging* **36**, 68–80 (2015).
16. Palmer, A. M. The activity of the pentose phosphate pathway is increased in response to oxidative stress in Alzheimer's disease. *J. Neural Transm. (Vienna)* **106**, 317–328 (1999).
17. Saharan, S. & Mandal, P. K. The emerging role of glutathione in Alzheimer's disease. *J. Alzheimer's Dis.***40**, 519–529 (2014).
18. Paglia, G. et al. Unbiased metabolomic investigation of Alzheimer's disease brain points to dysregulation of mitochondrial aspartate metabolism. *J. Proteome Res.* **15**, 608–618 (2016).
19. Griffin, J. W. & Bradshaw, P. C. Amino acid catabolism in Alzheimer's disease brain: friend or foe?. *Oxid. Med Cell Longev.* **2017**, 5472792 (2017).
20. Babygirija, R. et al. Protein restriction slows the development and progression of pathology in a mouse model of Alzheimer's disease. *Nat. Commun.* **15**, 5217 (2024).
21. Patel, N. S. et al. Inflammatory cytokine levels correlate with amyloid load in transgenic mouse models of Alzheimer's disease. *J. Neuroinflamm.* **2**, 9 (2005).
22. Meraz-Rios, M. A., Toral-Rios, D., Franco-Bocanegra, D., Villeda-Hernandez, J. & Campos-Pena, V. Inflammatory process in Alzheimer's Disease. *Front Integr. Neurosci.* **7**, 59 (2013).
23. Bonow, R. H., Aid, S., Zhang, Y., Becker, K. G. & Bosetti, F. The brain expression of genes involved in inflammatory response, the ribosome, and learning and memory is altered by centrally injected lipopolysaccharide in mice. *Pharmacogenomics J.* **9**, 116–126 (2009).
24. Castillo, E. et al. Comparative profiling of cortical gene expression in Alzheimer's disease patients and mouse models demonstrates a link between amyloidosis and neuroinflammation. *Sci. Rep.* **7**, 17762 (2017).
25. Talboom, J. S., Velazquez, R. & Oddo, S. The mammalian target of rapamycin at the crossroad between cognitive aging and Alzheimer's disease. *NPJ Aging Mech. Dis.* **1**, 15008 (2015).
26. Uddin, M. S. et al. Autophagic dysfunction in Alzheimer's disease: cellular and molecular mechanistic approaches to halt Alzheimer's pathogenesis. *J. Cell Physiol.* **234**, 8094–8112 (2019).
27. Simcox, J. & Lamming, D. W. The central moTOR of metabolism. *Dev. Cell* **57**, 691–706 (2022).
28. Muller, L. et al. Long-term caloric restriction attenuates beta-amyloid neuropathology and is accompanied by autophagy in APPswe/PS1delta9 Mice. *Nutrients* **13**, 985 (2021).
29. Duan, W., Lee, J., Guo, Z. & Mattson, M. P. Dietary restriction stimulates BDNF production in the brain and thereby protects neurons against excitotoxic injury. *J. Mol. Neurosci.* **16**, 1–12 (2001).
30. Kishi, T. et al. Calorie restriction improves cognitive decline via up-regulation of brain-derived neurotrophic factor: tropomyosin-related kinase B in hippocampus of obesity-induced hypertensive rats. *Int. Heart J.* **56**, 110–115 (2015).
31. Miranda, M., Morici, J. F., Zanoni, M. B. & Bekinschtein, P. Brain-derived neurotrophic factor: a key molecule for memory in the healthy and the pathological brain. *Front Cell Neurosci.* **13**, 363 (2019).
32. Phillips, H. S. et al. BDNF mRNA is decreased in the hippocampus of individuals with Alzheimer's disease. *Neuron* **7**, 695–702 (1991).
33. Connor, B. et al. Brain-derived neurotrophic factor is reduced in Alzheimer's disease. *Brain Res. Mol. Brain Res.* **49**, 71–81 (1997).
34. Hock, C., Heese, K., Hulette, C., Rosenberg, C. & Otten, U. Region-specific neurotrophin imbalances in Alzheimer disease: decreased levels of brain-derived neurotrophic factor and increased levels of nerve growth factor in hippocampus and cortical areas. *Arch. Neurol.* **57**, 846–851 (2000).
35. Peng, S. et al. Decreased brain-derived neurotrophic factor depends on amyloid aggregation state in transgenic mouse models of Alzheimer's disease. *J. Neurosci.* **29**, 9321–9329 (2009).
36. Ng, T. K. S., Ho, C. S. H., Tam, W. W. S., Kua, E. H., Ho, R. C. Decreased serum brain-derived neurotrophic factor (BDNF) levels in patients with Alzheimer's Disease (AD): a systematic review and meta-analysis. *Int. J. Mol. Sci.* **20**, 257 (2019).
37. Takei, N. et al. Brain-derived neurotrophic factor induces mammalian target of rapamycin-dependent local activation of translation machinery and protein synthesis in neuronal dendrites. *J. Neurosci.* **24**, 9760–9769 (2004).
38. Takei, N., Kawamura, M., Hara, K., Yonezawa, K. & Nawa, H. Brain-derived neurotrophic factor enhances neuronal translation by activating multiple initiation processes: comparison with the effects of insulin. *J. Biol. Chem.* **276**, 42818–42825 (2001).
39. Maswood, N. et al. Caloric restriction increases neurotrophic factor levels and attenuates neurochemical and behavioral deficits in a primate model of Parkinson's disease. *Proc. Natl. Acad. Sci. USA* **101**, 18171–18176 (2004).
40. Seidler, K. & Barrow, M. Intermittent fasting and cognitive performance - Targeting BDNF as potential strategy to optimise brain health. *Front Neuroendocrinol.* **65**, 100971 (2022).
41. Mattson, M. P. & Arumugam, T. V. Hallmarks of brain aging: adaptive and pathological modification by metabolic states. *Cell Metab.* **27**, 1176–1199 (2018).
42. Rothman, S. M. & Mattson, M. P. Activity-dependent, stress-responsive BDNF signaling and the quest for optimal brain health and resilience throughout the lifespan. *Neuroscience* **239**, 228–240 (2013).
43. Mihaylova, M. M. et al. When a calorie is not just a calorie: diet quality and timing as mediators of metabolism and healthy aging. *Cell Metab.* **35**, 1114–1131 (2023).
44. Lobo, F., Haase, J., Brandhorst, S. The effects of dietary interventions on brain aging and neurological diseases. *Nutrients* **14**, 5086 (2022).

45. Pan, R. Y. et al. Intermittent fasting protects against Alzheimer's disease in mice by altering metabolism through remodeling of the gut microbiota. *Nat. Aging* **2**, 1024–1039 (2022).
46. Lv, R. et al. Intermittent fasting and neurodegenerative diseases: Molecular mechanisms and therapeutic potential. *Metabolism* **164**, 156104 (2025).
47. Wu, L. et al. Intermittent fasting ameliorates beta-amyloid deposition and cognitive impairment accompanied by decreased lipid droplet aggregation within microglia in an Alzheimer's disease model. *Mol. Nutr. Food Res.* **69**, e202400660 (2025).
48. Anson, R. M. et al. Intermittent fasting dissociates beneficial effects of dietary restriction on glucose metabolism and neuronal resistance to injury from calorie intake. *Proc. Natl. Acad. Sci. USA* **100**, 6216–6220 (2003).
49. Arumugam, T. V. et al. Multiomics analyses reveal dynamic bioenergetic pathways and functional remodeling of the heart during intermittent fasting. *Elife* **12**, RP89214 (2023).
50. Hatori, M. et al. Time-restricted feeding without reducing caloric intake prevents metabolic diseases in mice fed a high-fat diet. *Cell Metab.* **15**, 848–860 (2012).
51. Jeong, M. A. et al. Intermittent fasting improves functional recovery after rat thoracic contusion spinal cord injury. *J. Neurotrauma* **28**, 479–492 (2011).
52. Hu, Y., Yang, Y., Zhang, M., Deng, M. & Zhang, J. J. Intermittent fasting pretreatment prevents cognitive impairment in a rat model of chronic cerebral hypoperfusion. *J. Nutr.* **147**, 1437–1445 (2017).
53. Liu, Y. et al. SIRT3 mediates hippocampal synaptic adaptations to intermittent fasting and ameliorates deficits in APP mutant mice. *Nat. Commun.* **10**, 1886 (2019).
54. Acosta-Rodriguez, V. et al. Circadian alignment of early onset caloric restriction promotes longevity in male C57BL/6J mice. *Science* **376**, 1192–1202 (2022).
55. Aon, M. A. et al. Untangling determinants of enhanced health and lifespan through a multi-omics approach in mice. *Cell Metab.* **32**, 100–116.e104 (2020).
56. Patel, N. V. et al. Caloric restriction attenuates Abeta-deposition in Alzheimer transgenic models. *Neurobiol. Aging* **26**, 995–1000 (2005).
57. Mehta, D., Jackson, R., Paul, G., Shi, J. & Sabbagh, M. Why do trials for Alzheimer's disease drugs keep failing? A discontinued drug perspective for 2010-2015. *Expert Opin. Investig. Drugs* **26**, 735–739 (2017).
58. Zhang, Y., Chen, H., Li, R., Sterling, K. & Song, W. Amyloid beta-based therapy for Alzheimer's disease: challenges, successes and future. *Signal Transduct. Target Ther.* **8**, 248 (2023).
59. Javonillo, D. I. et al. Systematic phenotyping and characterization of the 3xTg-AD mouse model of Alzheimer's disease. *Front Neurosci.* **15**, 785276 (2021).
60. Gawel, K., Gibula, E., Marszalek-Grabska, M., Filarowska, J. & Kotlinska, J. H. Assessment of spatial learning and memory in the Barnes maze task in rodents-methodological consideration. *Naunyn Schmiedebergs Arch. Pharm.* **392**, 1–18 (2019).
61. Illouz, T., Ascher, L. A. B., Madar, R. & Okun, E. Unbiased analysis of spatial learning strategies in a modified Barnes maze using convolutional neural networks. *Sci. Rep.* **14**, 15944 (2024).
62. Harrison, F. E., Reiserer, R. S., Tomarken, A. J. & McDonald, M. P. Spatial and nonspatial escape strategies in the Barnes maze. *Learn Mem.* **13**, 809–819 (2006).
63. Stevens, L. M. & Brown, R. E. Reference and working memory deficits in the 3xTg-AD mouse between 2 and 15-months of age: a cross-sectional study. *Behav. Brain Res.* **278**, 496–505 (2015).
64. Stover, K. R., Campbell, M. A., Van Winssen, C. M. & Brown, R. E. Early detection of cognitive deficits in the 3xTg-AD mouse model of Alzheimer's disease. *Behav. Brain Res.* **289**, 29–38 (2015).
65. Tramutola, A., Lanzillotta, C. & Di Domenico, F. Targeting mTOR to reduce Alzheimer-related cognitive decline: from current hits to future therapies. *Expert Rev. Neurother.* **17**, 33–45 (2017).
66. Wilkinson, J. E. et al. Rapamycin slows aging in mice. *Aging Cell* **11**, 675–682 (2012).
67. Cogut, V., McNeely, T. L., Bussian, T. J., Graves, S. I. & Baker, D. J. Caloric Restriction improves spatial learning deficits in tau mice. *J. Alzheimer's Dis.: JAD* **98**, 925–940 (2024).
68. Wu, P. et al. Calorie restriction ameliorates neurodegenerative phenotypes in forebrain-specific presenilin-1 and presenilin-2 double knockout mice. *Neurobiol. Aging* **29**, 1502–1511 (2008).
69. Bejanin, A. et al. Tau pathology and neurodegeneration contribute to cognitive impairment in Alzheimer's disease. *Brain* **140**, 3286–3300 (2017).
70. Brownlow, M. L. et al. Partial rescue of memory deficits induced by calorie restriction in a mouse model of tau deposition. *Behav. Brain Res.* **271**, 79–88 (2014).
71. Wang, L. et al. Methionine restriction alleviates high-fat diet-induced obesity: Involvement of diurnal metabolism of lipids and bile acids. *Biochim Biophys. Acta Mol. Basis Dis.* **1866**, 165908 (2020).
72. Gao, X. et al. Dietary methionine influences therapy in mouse cancer models and alters human metabolism. *Nature* **572**, 397–401 (2019).
73. Yu, D. et al. Short-term methionine deprivation improves metabolic health via sexually dimorphic, mTORC1-independent mechanisms. *FASEB J.* **32**, 3471–3482 (2018).
74. Zhao, Y. et al. Blood levels of circulating methionine components in Alzheimer's disease and mild cognitive impairment: A systematic review and meta-analysis. *Front Aging Neurosci.* **14**, 934070 (2022).
75. Xi, Y. et al. Effects of methionine intake on cognitive function in mild cognitive impairment patients and APP/PS1 Alzheimer's Disease model mice: Role of the cystathionine-beta-synthase/H(2)S pathway. *Redox Biol.* **59**, 102595 (2023).
76. Haws, S. A., Leech, C. M. & Denu, J. M. Metabolism and the epigenome: a dynamic relationship. *Trends Biochem Sci.* **45**, 731–747 (2020).
77. Haws, S. A. et al. Dietary restriction of individual amino acids stimulates unique molecular responses in mouse liver. *bioRxiv*, (2023).
78. Mentch, S. J. et al. Histone methylation dynamics and gene regulation occur through the sensing of one-carbon metabolism. *Cell Metab.* **22**, 861–873 (2015).
79. Zhang, N. Role of methionine on epigenetic modification of DNA methylation and gene expression in animals. *Anim. Nutr.* **4**, 11–16 (2018).
80. Lardenoije, R. et al. Age-related epigenetic changes in hippocampal subregions of four animal models of Alzheimer's disease. *Mol. Cell Neurosci.* **86**, 1–15 (2018).
81. Chouliaras, L. et al. Consistent decrease in global DNA methylation and hydroxymethylation in the hippocampus of Alzheimer's disease patients. *Neurobiol. Aging* **34**, 2091–2099 (2013).
82. Chouliaras, L. et al. Epigenetic regulation in the pathophysiology of Alzheimer's disease. *Prog. Neurobiol.* **90**, 498–510 (2010).
83. Collet, T. H. et al. A metabolomic signature of acute caloric restriction. *J. Clin. Endocrinol. Metab.* **102**, 4486–4495 (2017).
84. Bellantuono, I. et al. A toolbox for the longitudinal assessment of healthspan in aging mice. *Nat. Protoc.* **15**, 540–574 (2020).
85. Pak, H. H. et al. Non-canonical metabolic and molecular effects of calorie restriction are revealed by varying temporal conditions. *Cell Rep.* **43**, 114663 (2024).
86. Small, L. et al. Comparative analysis of oral and intraperitoneal glucose tolerance tests in mice. *Mol. Metab.* **57**, 101440 (2022).

87. Sonsalla, M. M. & Lamming, D. W. Geroprotective interventions in the 3xTg mouse model of Alzheimer's disease. *Geroscience* **45**, 1343–1381 (2023).
88. Ruhlmann, C. et al. Long-term caloric restriction in ApoE-deficient mice results in neuroprotection via Fgf21-induced AMPK/mTOR pathway. *Aging (Albany NY)* **8**, 2777–2789 (2016).
89. Cohen, H. Y. et al. Calorie restriction promotes mammalian cell survival by inducing the SIRT1 deacetylase. *Science* **305**, 390–392 (2004).
90. Madeo, F., Carmona-Gutierrez, D., Hofer, S. J. & Kroemer, G. Caloric restriction mimetics against age-associated disease: targets, mechanisms, and therapeutic potential. *Cell Metab.* **29**, 592–610 (2019).
91. Kaur, H., Seeger, D., Golovko, S., Golovko, M., Combs, C. K. Liver bile acid changes in mouse models of Alzheimer's disease. *Int. J. Mol. Sci.* **22**, 7451 (2021).
92. Bosoi, C. R. et al. High-fat diet modulates hepatic amyloid beta and cerebrosterol metabolism in the triple transgenic mouse model of Alzheimer's disease. *Hepatol. Commun.* **5**, 446–460 (2021).
93. Bassendine, M. F., Taylor-Robinson, S. D., Fertleman, M., Khan, M. & Neely, D. Is Alzheimer's disease a liver disease of the brain?. *J. Alzheimer's Dis.* **75**, 1–14 (2020).
94. Rigby, M. J. et al. Endoplasmic reticulum acetyltransferases Atase1 and Atase2 differentially regulate reticulophagy, macroautophagy and cellular acetyl-CoA metabolism. *Commun. Biol.* **4**, 454 (2021).
95. Pang, Z. et al. MetaboAnalyst 6.0: towards a unified platform for metabolomics data processing, analysis and interpretation. *Nucleic Acids Res.* **52**, W398–W406 (2024).

Acknowledgements

We would like to thank Dr. Heidi Pak for her valuable insights and support. We thank all the members of the Lamming lab for their feedback. The Lamming lab is supported in part by the NIA (AG056771, AG062328, AG061635, AG081482, AG084156, and AG094153 to D.W.L.), the NIDDK (DK125859 to D.W.L. and J.M.D.), by a grant from the Alzheimer's Association (23AARG-1029665 to D.W.L.), and by startup funds from UW-Madison. This study was supported in part by F31AG081115 (to R.B.), Supplement to Promote Diversity in Health-Related Research RF1AG056771-06S1 (to M.M.S.), Dalio Philanthropies, a Glenn Foundation for Medical Research Postdoctoral Fellowship, and by grant HF-AGE AGE-009 from the Hevolution Foundation to C.L.G.; M.F.C. was supported in part by F31 AG082504 (to M.F.C.). C.Y.Y. was supported in part by NIA F32 postdoctoral fellowship (F32AG077916 to C.Y.Y.) and a NIA K99 award (K99AG084921 to C.Y.Y.). The Puglielli lab is supported in part by the NINDS (NS094154 to L.P.), the NIGMS (GM148487 to L.P.) and the NIA (AG078794 to L.P.). The Harris lab is supported by the UW Department of Surgery, School of Medicine and Public Health, Wisconsin Alumni Research Fund, and the Office of the Vice Chancellor for Research. Additionally, the Harris lab has funding through the NIA (R03AG088813 to D.A.H.), Wisconsin Alzheimer's Disease Research Center (P30 AG062715), and a grant from the Wisconsin Partnership Program at the UW School of Medicine and Public Health (ID 6770-2024 to D.A.H.). The Denu lab is supported in part by the NIH (GM149279 and DK125859 to J.M.D.). The authors thank the University of Wisconsin Carbone Cancer Center Experimental Animal Pathology Laboratory supported by P30 CA014520, for use of its facilities and services. L.P., D.A.H., J.M.D. and D.W.L. are members of the Wisconsin Nathan Shock Center of Excellence in the Basic Biology of Aging, P30 AG092586. The Lamming lab was supported in part by the U.S. Department of Veterans Affairs (I01-BX004031 and IS1-BX005524 to D.W.L.), and this work was supported using facilities and resources from the William S. Middleton Memorial Veterans Hospital. The content is solely the responsibility of the authors and does not necessarily represent the official views of the NIH. This work does not represent the views of the Department of Veterans Affairs or the United States Government.

Author contributions

R.B., J.H.H., M.M.S., R.M., M.F.C., C.L.G., A.T., C.Y.Y., S.S., J.I., Y.L., and I.G. conducted the experiments. R.B., J.H.H., C.L.G., D.V. and D.W.L. analyzed the data. R.B., J.H.H., M.J.R., D.A.H., J.M.D., L.P., and D.W.L. wrote and edited the manuscript.

Competing interests

D.W.L. has received funding from, and is a scientific advisory board member of, Aeovian Pharmaceuticals, which seeks to develop novel, selective mTOR inhibitors for the treatment of various diseases. J.M.D. is a consultant for Evrys Bio and co-founder of Galilei BioSciences. The remaining authors declare no competing interests.

Additional information

Supplementary information The online version contains supplementary material available at https://doi.org/10.1038/s41467-025-62416-3.

Correspondence and requests for materials should be addressed to Dudley W. Lamming.

Peer review information *Nature Communications* thanks Mark Mattson, and the other, anonymous, reviewer(s) for their contribution to the peer review of this work. A peer review file is available.